

A caspase-dependent pathway regulates microglia activation and neurotoxicity

Miguel A. Burguillos^{1,2,3}, Tomas Deierborg^{3#}, Edel Kavanagh^{1#}, Annette Persson⁴, Nabil Hajji^{1,†}, Albert Garcia-Quintanilla^{2,5}, Josefina Cano², Patrik Brundin³, Elisabet Englund⁴, Jose L. Venero^{2,*}, and Bertrand Joseph^{1,*}.

¹ Department of Oncology-Pathology, Cancer Centrum Karolinska, Karolinska Institutet, SE-171 77, Stockholm, Sweden

² Departamento de Bioquímica y Biología Molecular, Facultad de Farmacia, Universidad de Sevilla, and Instituto de Biomedicina de Sevilla, 41012 Sevilla, Spain

³ Neuronal Survival Unit, Wallenberg Neuroscience Center, Department of Experimental Medical Science, 221 84 Lund, Sweden

⁴ Department of Pathology, Division of Neuropathology, Lund University Hospital, 221 85 Lund, Sweden.

⁵ Servicio de Biología, Centro de Investigación, Tecnología e Innovación, Universidad de Sevilla (CITIUS), 41012 Sevilla, Spain

* Present address: Department of Experimental Medicine and Toxicology, Division of Investigative Science, Imperial College London, United Kingdom

*J.L.V and B.J share senior authorship.

T.D and E.K share second authorship.

Correspondence to: Jose Luis Venero², and Bertrand Joseph¹. Correspondence and requests for materials should be addressed to J.L.V. (Email: jlvenero@us.es) or B.J. (Email: bertrand.joseph@ki.se)

Summary

Activation of microglia and inflammation-mediated neurotoxicity are suggested to play a decisive role in the pathogenesis of several neurodegenerative disorders. Activated microglia release pro-inflammatory factors that may be neurotoxic. Here we show that the orderly activation of caspase-8 and caspase-3/7, known executioners of apoptotic cell death, regulate microglia activation via a PKC δ -dependent pathway. We found that stimulation of microglia with various inflammogens activates caspase-8 and caspase-3/7 in microglia without triggering cell death *in vitro* and *in vivo*. Knockdown or chemical inhibition of each of these caspases hindered microglia activation and consequently reduced neurotoxicity. We also observed that these caspases are activated in microglia in the ventral mesencephalon of Parkinson's disease and the frontal cortex of Alzheimer's disease subjects. Taken together we show that caspase-8 and caspase-3/7 are involved in regulating microglia activation. We conclude that inhibition of these caspases could be neuroprotective by targeting the microglia rather than the neurons themselves.

Introduction

Numerous *in vivo* clinical imaging and neuropathology studies suggest that activated microglia, the resident immune cells of the central nervous system (CNS), play prominent roles in the pathogenesis of neurodegenerative disorders, including Parkinson's disease (PD), multiple sclerosis and Alzheimer's disease (AD)^{1,2}. Microglia are necessary for normal brain function, however, uncontrolled and over-activated microglia can trigger neurotoxicity. They are a prominent source of pro-inflammatory factors and oxidative stress such as tumor necrosis factor (TNF) α , nitric oxide (NO) and Interleukin (IL)-1 β , which are neurotoxic²⁻⁴.

Toll-like receptors (TLRs) are a family of pattern-recognition receptors in the innate immune system. Exogenous and endogenous TLR ligands activate microglia^{1,5}. Intracerebral delivery of lipopolysaccharide (LPS), the major component of Gram negative bacterial walls and a ligand for TLR4, leads *in vivo* to microglia activation and neuronal injury, and is used as model for brain inflammation^{6,7}. Synergistic effects between interferon-gamma (IFN γ) and several TLR ligands (including TLR4) have been suggested, suggesting crosstalk between these pro-inflammatory receptor signaling pathways⁸. Furthermore, IFN γ receptor-deficient mice are less susceptible to LPS-induced endotoxic shock than control mice⁹. Finally, TLR4 has been implicated in AD pathophysiology in several contexts. Thus, the upregulation of cytokines is TLR4-dependent in an AD mouse model¹⁰; certain TLR4 single nucleotide polymorphisms are associated with increased risk for AD¹¹; the levels of TLR4 mRNA are upregulated in APP transgenic mice¹²; and increased TLR4 expression is associated with amyloid plaque deposition in AD brain tissue¹².

Caspases, a family of cysteinyl aspartate-specific proteases, are executioners of apoptotic cell death and their activation is considered a commitment to cell death^{13,14}. Certain caspases, *e.g.* caspase-1, also play a pivotal role in immune-mediated inflammation. In this situation, caspase activation is associated with the maturation of pro-inflammatory cytokines, such as interleukin-1beta (IL-1beta), IL-18, IL-33, and not with apoptosis¹⁵. Inhibition of caspase activation protects against

neuronal loss in several animal models of brain diseases involving activated microglia, including hypoxic ischemia/stroke, acute bacterial meningitis, brain trauma and 6-hydroxydopamine and 1-methyl-4-phenyl-1,2,3,6-tetrahydropyridine (MPTP)-lesioned parkinsonism models^{2,16-20}. Presently, it is unclear whether inhibition of caspase activation specifically in microglia contributes to the neuroprotective effects of caspase inhibitors. We have now discovered that microglial activation in cell and animal models of inflammation involves caspases and that specific inhibition of the cascade in microglia prevents neurodegeneration. Furthermore, we demonstrate that caspase activation occurs in microglia in the brains of subjects with PD and AD, and thereby we validate the observations we made in relevant cell and animal models.

Results

LPS-induced caspase-3/7 activity regulates microglia activation.

We stimulated BV2 cells with LPS to investigate the molecular pathways involved in microglia activation (Fig. 1). LPS treatment induced caspase-3 cleavage and D(OMe)E(OMe)VD(OMe)-ase (DEVD-ase) activity after only 4 h in BV2 microglia cells in a time and dose-dependent manner (Fig. 1a, e and supplementary Fig. 1a-b and e-f and Fig. 4d). Increased DEVD-ase activity was also observed upon treatment with other pro-inflammogens such as Lipoteichoic acid (LTA, TLR2 agonist), PamC3sk4 (synthetic lipopeptide TLR1/2 agonist) and interferon-gamma (IFN γ) (supplementary Fig. 2a). This activity primarily reflects caspase-3/7 activities. Both caspase 3 and 7 are known as major apoptosis executioners. Despite the increase in DEVD-ase activity, we did not observe major microglia cell death within the first 24 h after initiating LPS treatment (Fig. 1c and supplementary Fig. 1c and Fig. 3a-c, e-f) nor with LTA, PamC3sk4 and IFN γ treatments (supplementary Fig. 2b-c). Thus, the LPS-induced increase in caspase 3 and 7 activity did not result in major cell death and the little cell death occurring at 48 h

was not prevented using the specific caspase-3/7 inhibitor Z-D(OMe)E(OMe)VD(OMe)-FMK (DEVD-fmk) (supplementary Fig. 1d and supplementary Fig. 3d and g). As compared to LPS treatment, exposure of BV2 microglia cells to a death stimulus such as staurosporine (STS) led to a significantly greater caspase-3 cleavage and induction of DEVD-ase activity (Fig. 1a and e and supplementary Fig. 4d). Following LPS treatment, we found cleaved caspase-3 to be located primarily close to the plasma membrane and not present in the nucleus (Fig. 1b and supplementary Fig. 4a-d, Movies 1 and 2). Furthermore, we did not observe cleavage of the caspase-3/7 nuclear substrate Poly(ADP-ribose) polymerase (PARP-1) in response to LPS (Fig. 1d) even after long exposure of the membrane (Fig. 1d*). In addition, whereas exposure of BV2 cells to STS promoted Bid processing and loss of mitochondrial transmembrane potential, these two events associated with the mitochondrial cell death pathway were found to be unaffected upon LPS treatment (Fig. 1f-g). When we inhibited DEVD-ase activity in BV2 cells by exposing them to the cell-permeable and irreversible caspase inhibitor DEVD-fmk, LPS treatment failed to activate the microglia. Thus, the cells did not exhibit morphological changes associated with microglia activation (Fig. 1h-i) and did not show features of activated microglia, such as IKK β , iNOS and ROS formation (Fig. 1j-m). Co-treatment with DEVD-fmk also prevented the LTA, Pam3CSK4 and IFN γ -induced iNOS expression and ROS formation (supplementary Fig. 5a-e). Caspase-3 and -7 account for cellular DEVD-ase activity. We therefore decided to assess their respective roles in microglia activation by selectively knocking down endogenous caspase-3 (supplementary Fig. 6a-b) or caspase-7 (supplementary Fig. 6c-d) using a pool of small interfering RNAs (siRNAs). First, we confirmed that the silencing of these proteases effectively decreased DEVD-ase activity (supplementary Fig. 6e). Then, when we transfected BV2 microglia cells with siRNA targeting specifically either one of the two caspases, LPS-treatment did not induce iNOS, IKK β expression, ROS formation and production of certain cytokine production (IL1- β , TNF- α and mKC) as effectively (Fig. 2a-b and supplementary Fig.

6f-i). We found that silencing both caspases simultaneously reduced IKK β expression even further (supplementary Fig. 6f). This indicates that DEVD-ase activity *per se* regulates microglia activation (Fig. 2 and supplementary Fig. 6). Similar responses to caspase-3 and -7 knockdowns were observed with LTA, Pam3CSk4 and IFN γ treatments (supplementary Fig. 7a-i). Activation and nuclear translocation of nuclear factor κ B (NF- κ B) is a key step in LPS-induced microglia activation²¹. NF- κ B is sequestered in the cytoplasm by the I κ B family of inhibitory proteins that mask the nuclear localization signal of NF- κ B. IKK β can phosphorylate I κ B, and thereby target it for degradation via the ubiquitin proteasome pathway. As a consequence, functional NF- κ B molecules then become free to enter the nucleus. We detected less nuclear NF- κ B p65 subunits in cells subjected to knockdown of caspase-3 or caspase-7 prior to LPS treatment (Fig. 2c-d), indicating that reduced caspase activation led to less nuclear translocation of NF- κ B. Finally, using microglia cells co-cultured with dopaminergic neurons, we examined whether the inhibition of the IKK/NF- κ B pathways by selective knockdown of caspase-3 or/and capase-7 was associated with loss of microglia neurotoxicity. In agreement with earlier studies^{22,23}, LPS treatment activated microglia and caused dopaminergic neurons to die. Importantly, we found that reducing the LPS-induced microglia activation by caspase knockdown meant that fewer co-cultured dopaminergic neurons died (Fig. 2e-f). Also, we checked the level of several cytokines in primary microglial cell cultures at 12 and 24h, and observed a decrease of IL-1 β and IL-5 with both DEVD-fmk and IETD-fmk, and also of IL-2 and IFN γ at 12h when we used IETD-fmk (Fig. 2g).

Caspase-8 but not caspase-1 activity controls LPS-induced caspase-3/7 activation.

We then examined how caspase-3/7 are activated in LPS-treated microglia. LPS treatment has been reported to promote caspase-1 activation²⁴. Caspase 1 is a key component of the inflammasome required for the processing and maturation of pro-

inflammatory cytokines. It plays a pivotal role during LPS-induced inflammation. Therefore caspase-1 null mice and mice expressing a dominant-negative mutant caspase-1 gene exhibit reduced LPS-induced inflammation^{25,26}. Consequently, we examined if caspase-1 acts upstream of caspase-3/-7 in LPS-induced microglia activation. We found that the specific caspase-1 inhibitor YVAD-fmk did not reduce LPS-induced activation of microglia, as assessed by DEVD-ase activity (Fig. 3a). Caspase-8 is believed to be at the apex of the death receptor-mediated apoptosis pathway and can activate caspase-3/-7²⁷⁻²⁹. We found that LPS induced caspase-8 activity (IETD-ase) within 6 h of being added to BV2 microglia cultures (Fig. 3b-c). Consistent with this result, we observed that the specific caspase-8 inhibitor IETD-fmk or caspase-8 knockdown using siRNA prevented LPS-induced DEVD-ase activity (Fig. 3a, d). The IETD-fmk treatment or caspase-8 silencing only prevented the LPS-induced increase in DEVD-ase activity, whereas the caspase inhibitor DEVD-fmk reduced the DEVD-ase activity even further (Fig. 3a, c). Knockdown or chemical inhibition of caspase-8 were also associated with a reduction of iNOS expression and ROS formation upon treatment with all tested pro-inflammogens (*i.e.* LPS, LTA, Pam3CSK4 and IFN γ) (Fig. 3e-h and supplementary Fig. 6i, Fig. 7a-i and 8a-b). Other known potential caspase-8 substrates *i.e.* Bid, HDAC7 and RIP1 were found to not be processed upon LPS treatment. (Fig. 1f and supplementary Fig. 9). Taken together, this indicates that the LPS-induced increase in DEVD-ase activity is dependent on caspase-8 activation. Furthermore, we found that the caspase-8- and caspase-1-initiated pathways had additive effects concerning the regulation of LPS-induced iNOS expression (Fig. 3e-f). This suggests that both of these caspase-regulated pathways contribute to LPS-induced inflammation. We also examined if the observed DEVD-ase activity and that of caspase 6, the remaining executioner caspase, were correlated. However, we were unable to detect any VEID-ase activity (related to caspase-6) in cells upon LPS treatment. Pretreatment with VEID-fmk, a caspase 6 inhibitor, did not affect LPS-induced DEVD-ase activity,

indicating that this protease does not play an essential role in the activation process (supplementary Fig. 10a-b).

Activation of caspase-8 and caspase-3 is dependent on TLR4 but independent of MyD88 and TNFR1 signalling.

We then examined further the link between TLR4 ligation and activation of caspase-8. Selective knockdown of TLR4 (supplementary Fig. 11a) was associated with a reduced caspase-8 activation and consequent caspase-3 activation providing evidence for a direct activation of caspase-8 by TLR4 ligation (supplementary Fig. 11b-c). Apoptosis following TLR2 activation has been reported to be associated to the formation of a myeloid differentiation factor 88 (MyD88)/ Fas-associated death domain protein (FADD)/Caspase-8 complex³². In order to assess the potential role of this complex in TLR4 ligation induced microglia activation, we knocked down MyD88 by siRNAs (supplementary Fig. 11d). We observed that down-regulation of MyD88 did not affect LPS-induced activation of caspase-3 and caspase-8 (supplementary Fig. 11e-f), suggesting that TLR4 ligation-induced microglia activation did not act through recruitment of the MyD88/FADD/caspase-8, as is the case for TLR2 ligation-induced apoptosis^{32,33}.

Microglia activation can be regulated by autocrine signalling of TNF α via the TNF receptor 1 (TNFR1) secreted by LPS-stimulated microglia³⁴. To examine whether we were observing a secondary effect, induced by autocrine signalling of TNF α excreted by LPS-stimulated microglia cells, we investigated the effect of neutralizing TNF α Receptor antibodies on LPS-induced caspase-3 and caspase-8 activities³⁴ (supplementary Fig. 12a-d). Selectively blocking the TNF α receptor resulted in decreased LPS-induced iNOS expression at 24h, thus confirming the TNF α positive feedback loop exerted on microglia cells (supplementary Fig. 12e). However, it failed to affect the LPS-induced caspase-3 and caspase-8 activities (supplementary Fig. 12a-d). Thus, this experiment demonstrates that the caspase-signaling

pathway is directly activated, independently of TNF α receptor stimulation, upon LPS treatment.

Caspase-3/7 regulates microglia activation via PKC δ pathway.

We then explored how activated caspase-3/-7 interacts with the IKK/NF- κ B pathway during LPS-induced microglia activation. Protein kinase C- δ (PKC δ) has been reported to regulate NF- κ B activation through the IKK complexes and phosphorylation of the NF- κ B inhibitor I κ B³³⁻³⁵. Interestingly, PKC δ can be cleaved by caspases to generate a 40kDa catalytically active fragment³⁶. Since the levels of this protein are quite low in this cell line, we decided to overexpress PKC δ in order to detect the cleaved form (Fig. 4a). We found that LPS treatment of BV2 microglia cells promoted cleavage of PKC δ into its 40kDa active fragment (Fig. 4b-c). We found that the caspase inhibitor DEVD-fmk or selective siRNA knockdown of caspase-3 or caspase-7 reduced LPS-induced PKC δ activation. Therefore, in this context, PKC δ activation is dependent on DEVD-ase activity (Fig. 4b-e). We then obtained further evidence supporting that PKC δ activation is important in microglia activation. First, we found that the PKC δ inhibitor rottlerin inhibits LPS-induced iNOS expression in microglia (Fig. 4f-g). Second, if we over-expressed in microglia cells a caspase uncleavable mutant of PKC δ , we observed a decrease of LPS-induced iNOS expression (Fig. 4h-i). By contrast, when we over-expressed PKC δ , we further enhanced the activating effect of LPS on microglia (supplementary Fig. 13). Also, we observed a marked decrease of all cytokines in primary microglial cell cultures after being challenged with rottlerin (Fig. 4j). Taken together, our experiments demonstrate that the caspase-3/7-dependent activation of microglia by LPS is mediated through PKC δ .

***In vivo* inhibition of the caspase-dependent pathway prevents LPS-induced microglia activation.**

To examine the physiological relevance of these findings, we performed *in vivo* experiments and injected LPS into the rat substantia nigra (SN). The SN is known to exhibit a strong inflammatory response upon LPS challenge⁶. At 24 hours post-injection (Fig. 5a-c), we observed a strong induction of caspase-8 and activation of caspase-3, which was mostly confined to reactive microglia in the mesencephalon on the injected side (Fig. 5b-c). By contrast, microglia were quiescent in the contralateral control midbrain (Fig. 5a). To study if caspase-3/7 activation is important for microglia activation also *in vivo*, we co-injected DEVD-fmk with LPS. Twenty-four hours later, we found that caspase-3/7 inhibition prevented LPS-induced microglia activation (Fig. 5d-e). At the molecular level, we observed that the DEVD-fmk treatment mitigated LPS-induced expression of cytokines and pro-inflammatory molecules including iNOS, TNF α and IL-1 β (Fig. 5f). As a final step, we examined if our earlier *in vitro* findings concerning the role of PKC δ in caspase-mediated microglia activation are relevant to the *in vivo* situation. We injected LPS intranigally together with IETD-fmk, DEVD-fmk or rottlerin. Twenty hours later, we dissected the SN and measured the iNOS protein level. In agreement with our *in vitro* data, we found that inhibition of caspase-8, caspase-3/7 or PKC δ activities significantly decreased LPS-induced iNOS expression (Fig. 5g-h).

Inhibition of caspase-8 decreases microglial activation and confers protection in an acute MPTP mouse model of PD.

To further substantiate our observations in the rat LPS model, we monitored the activation of microglia in the MPTP-lesion mouse model of PD. Consistent with earlier work, mice injected systemically with MPTP showed a strong microglial activation together with a robust neurotoxicity in ventral mesencephalic dopamine neurons³⁷. Intranigral vehicle injections in sham animals (saline containing 1% DMSO) greatly increased the density of reactive microglia, as evidenced by Iba1 immunohistochemistry (supplementary Fig. 14a-b). Consequently, we quantified the numbers of reactive and resting microglia in Iba1-immunostained sections

covering injection and non-injection sites for each experimental condition (Fig. 5i-j and supplementary Fig. 14a-b). As expected, the density of reactive microglia at the non-injection site was highest in the MPTP group and dramatically lower in the sham (no MPTP) group. Interestingly, caspase 8 inhibition significantly prevented the MPTP-induced microglia activation and the MPTP-induced reduction in the density of resting microglia (Fig. 5i-j). Similar results of IETD-fmk were observed at the injection site (supplementary Fig. 14a-b). As expected, MPTP injections severely reduced the integrity of nigro-striatal dopaminergic terminals (supplementary Fig. 14c-e). Intranigral IETD-fmk injection induced a modest, but significant, protection against MPTP-induced toxicity as demonstrated by densitometric analysis of surviving striatal dopaminergic terminals and stereological cell counts in the SN (supplementary Fig. 14c-e).

Activation of caspase-3 and caspase-8 in microglia in substantia nigra from PD and frontal cortex from AD subjects.

Parkinson's and Alzheimer's disease are known to be associated with neuroinflammation and the presence of activated microglia^{2,3}. We investigated whether caspase-3 and caspase-8 are activated in microglia of PD and AD subjects. We analysed expression of cleaved caspase-3, cleaved caspase-8 and the microglia marker CD68 in post-mortem brain samples from PD and AD subjects (clinically as well as neuropathologically diagnosed) and age- and gender-matched healthy control brains. We detected significant cytoplasmic expression of both active caspase-3 and active caspase-8 in the PD ventral mesencephalon and in the AD frontal cortex, compared to controls (Fig. 6a-d and supplementary Fig. 15, 16, 17, 18). The activated caspases and the microglial marker CD68 were largely co-localised, indicating that caspase-8 and caspase-3 are activated mainly in microglia in PD and AD (Fig. 6 a-d and supplementary Fig. 19a-b).

Discussion

In this study, we uncover a completely novel role for caspase-8 and caspase-3/7 in the control of microglia and brain inflammation. We show that stimulation of microglia with the pro-inflammatory stimuli LPS, LTA, Pam3CSK4 and IFN γ triggers caspase-3/7 activation, without causing cell death. Caspases are proteases essential for apoptosis and inflammation. Caspase-1 is already known as the prototypical inflammatory caspase, required for the maturation of pro-inflammatory cytokines. By comparison, the initiator caspase-8 and effector pro-apoptotic caspase-3 and caspase-7 are considered crucial in the intracellular death machinery. Unexpectedly, we showed that caspase-3/7 dependent DEVD-ase activity controls LPS induced-microglia activation. We demonstrated that inhibition of the caspase-3/7 pathway effectively block microglia activation. For example, we observed fewer microglia with an activated phenotype in the presence of the caspase inhibitor DEVD-fmk and inhibition of the downstream IKK/NF-kB pathways. We also reveal that caspase-3/7 activates the IKK/NF-kB pathways through processing and activation of PKC δ . Furthermore, we found that microglia exposed to the pro-inflammatory agent LPS failed to be toxic to neighbouring neurons when we inhibited caspase-3/7 chemically or by siRNA gene silencing. Importantly, we provide compelling evidence that active caspases 3 and 8 are expressed within reactive microglia in the ventral mesencephalon and frontal cortex of PD and AD subjects, respectively.

To summarize, we present new non-apoptotic functions for caspases-8, -3 and -7 and show that they can have a pivotal role in CNS inflammation (Fig. 6e). Brain inflammation is a typical feature of neurodegenerative diseases^{1,2,38} and is also a prominent sequel of many acute forms of brain injury (*e.g.* trauma, encephalitis and stroke)^{39,40}. Under certain circumstances, neuroinflammation is known to promote neuronal death⁴¹. Accordingly, previous studies have shown that anti-inflammatory treatment can reduce neurodegeneration. Our discovery that the caspases-8, -3 and -7 cascade can promote neuroinflammation via IKK/NF-kB and PKC δ , together with the development of nanocarriers that allow the inhibitor to

cross the blood brain barrier, opens up new molecular targets for anti-inflammatory drugs⁴². Considering that these caspases also regulate apoptotic neuronal death, our results should revitalize interest in caspase inhibitors as potential therapeutic agents in CNS disorders⁴³⁻⁴⁵.

Methods Summary

Microglial BV2 and dopaminergic MN9D murine cells were cultured as described^{46,47}. Experiments were performed in reduced 5% FCS media. Transfection of BV2 cells was carried out with Lipofectamine 2000 (Invitrogen). Non-targeting control, caspase-3, caspase-7 and caspase-8 siRNA were obtained from Dharmacon. Single and co-cultures were exposed to 1µg/ml LPS for the indicated time. Primary microglial cells were prepared from postnatal P1-3 mouse brain using a previously described protocol⁴⁸. Cytokine content in supernatants from primary microglia cultures exposed to 100ng/ml LPS were assayed using the Mouse TH1/TH2 9-PlexTissue Culture Kit (Meso-scale Discovery). DEVD-fmk (20µM), IETD-fmk (20µM), YVAD-fmk (20µM), rottlerin (2µM) or TNF R1 mouse Ab (20ng/ml) were added to the media 1h prior LPS treatment. Under approved protocols, male albino Wistar rats (230-250g) were intranigrally injected with 2µg LPS alone or in combination with 0.75nmol DEVD-fmk or 0.75nmol IETD-fmk. Rottlerin (20mg/kg) was administered intraperitoneally. Twenty-four hours post-surgery, rats were sacrificed and brains processed for analysis. Male C57BL mice were intranigrally injected with vehicle or 0.75nmol IETD-fmk. 12 hours later, animals were treated with four injections of MPTP (16mg/kg) at 2h intervals. Four days after the last injection, animals were sacrificed and brains processed for analysis. Paraffin-embedded archival tissue blocks from autopsy on three PD and three AD subjects were obtained from the Department of Pathology, Lund University Hospital, Sweden. Age matched control cases (cardiac arrest victims, no brain disease) were analysed at the same time. Histological, immunological and FACS analyses using

antibodies listed in [supplementary table 1](#) were performed using standard procedures^{46,49,50}. The subcellular localization of cleaved caspase-3, cleaved caspase-8, or NF- κ B p65 protein was determined by confocal microscopy. Quantitative PCR with primers listed in [supplementary table 2](#) were performed using SensiMixPlus SYBR (Quantace). MTT, caspase activity assay, apoptosis quantification and FACS analysis have been previously described⁴⁹. Statistical evaluations were performed by one or two-way ANOVA with Bonferroni post hoc tests and Kolmogorov-Smirnov test.

[Full methods](#) accompany this paper.

Online Methods

Reagents

LPS (from *Escherichia coli*, serotype 026:B6; Sigma), staurosporine (STS; Sigma), MPTP (Sigma), agonist anti-Fas monoclonal antibody clone CH11 (MBL), agonist anti-TNF α (R&D Systems) the caspase-3/7 inhibitor benzyloxycarbonyl-Asp(OMe)-Glu(OMe)-Val-Asp(OMe)-fluoromethylketone (DEVD-fmk), the caspase-8 inhibitor benzyloxycarbonyl-Ile-Glu(OMe)-Thr-Asp(OMe)-fluoromethylketone (IETD-fmk), the caspase-6 inhibitor benzyloxycarbonyl-Val-Glu(OMe)-Ile-Asp(OMe)-fluoromethylketone (VEID-fmk), the caspase-1 inhibitor benzyloxycarbonyl-Tyr-Val-Ala-Asp(OMe)-fluoromethylketone (YVAD-fmk; MP Biomedicals, Inc.) and the PKC δ inhibitor Rottlerin (Calbiochem) were used in this study. Plasmids encoding PKC δ and EGFP-PKC δ D327A were gifts of Dr L. Hjörstberg (Karolinska Institutet) and Dr M. Reyland (University of Colorado) respectively. ON-TARGET plus SMARTpools siRNAs were purchased from Dharmacon ([supplementary table 3](#)).

Animals and surgery

Animals used in this study were obtained from Center of Production and Animal Experimentation (Espartinas, Spain) and NMRI (Charles River, Germany). Experiments were performed in accordance with the Guidelines of the European

Union Council (86/609/EU), following Spanish and Swedish regulations for the use of laboratory animals and approved by the Scientific Committee of the University of Seville and Lund University. Intranigral injections were made 5.8mm anterior, 2.0mm lateral and 8.0mm ventral to the bregma in rat and 3.1mm anterior, \pm 1.2mm lateral and 5.1mm ventral from bregma in mouse.

Human brain

Human brain tissues from patients with PD of 5, 9 and 15 years' duration, respectively and age-matched control cases were used in this study⁵¹. The region investigated was the anterior mesencephalon covering the substantia nigra. Frontal cortex from AD patients of 4, 10 and 14 years' duration and controls were also used (Regional Ethical Review Board, Lund (Sweden) 2009-646/2010-25). The patients with dissimilar disease duration exhibited different degrees of severity of brain disease, reflecting different stages of the degenerative process. All sections were stained with haematoxylin-erythrosin and with antibodies against caspase 3, 8 and microglia, CD68 (see below). They were microscopically reviewed for verification of pathology. Prior to the investigation, the entire collection of brain sections, 15-20 per case including the mesencephalic section, were subjected to a neuropathological whole brain analysis for clinical diagnostic purpose, according to routine procedures at the department of Neuropathology. The project procedures involving human brain tissue were approved by the Regional Ethical Review Board in Lund, Sweden.

Co-culture and neuronal cell death assay

MN9D dopaminergic neuronal cells were stained with CellTracker™ Green CMFDA (Invitrogen) before BV2 microglia cells transfected with caspase-3 siRNA, caspase-7 siRNA or non-targeting siRNA were plated on them. After 24h, cells were treated with LPS and incubated for an additional 24h. They were then fixed with 4% paraformaldehyde and stained with 0.1mg/ml Hoechst for neuronal cell death quantification.

Primary cultures

Primary mouse microglial cells were plated for at least 48 h before the experiments (ethical permit M302-09). Cells were pretreated with inhibitors (20 μ M DEVD-fmk, 20 μ M IETD-fmk and 2 μ M Rottlerin one hour before with 100ng/ml LPS treatment).

Immunofluorescence and laser scanning confocal microscopy

Paraformaldehyde-fixed cells were blocked in PBS/3% goat serum/0.3% triton X-100 and incubated with the indicated primary (4°C, overnight) and AlexaFluor 488 or 594 conjugated anti-IgG used as secondary antibodies (RT, 1h; Molecular Probes). Nuclei were counterstained with DRAQ5TM (1 μ M, Alexis), Hoechst (1 μ g/ml, Molecular Probes) or DAPI (1 μ g/ml, Molecular Probes). Alexa 555-conjugated cholera toxin B (CTB; 10 μ g/mL; Molecular Probes) was used to stain lipid rafts on the plasma membrane. Protein subcellular localization was analyzed under Zeiss 510 META or Leica TCS-SP2 confocal laser scanning microscopy. The nuclear translocation of NF- κ B p65 subunit was quantified using multicolor 3D plug-in from Leica Confocal software and measured as the % of co-localization of DRAQ5TM with NF- κ B p65 inside the nucleus.

Fluorescence-activated cell sorting (FACS) analysis

Quantification of cells with cleaved caspase-3 and cleaved caspase-8 was performed with a FACScalibur flow cytometer (Becton Dickinson) using standard procedures. Analysis of data was performed using Cell Quest software.

Immunohistological and Immunohistochemistry

Rats and mice were perfused through the heart under deep anesthesia with 4% paraformaldehyde/PBS, pH 7.4. Brains were removed, cryoprotected in sucrose and frozen in isopentane at -15°C and serial coronal sections (25 μ M and 30 μ m sections, for rat and mice respectively) covering the striatum and the SN were cut with a cryostat and mounted on gelatin-coated slides. Sections were incubated with the indicated primary antibodies. After three washes, sections were then incubated with biotinylated horse anti-mouse or goat anti-rabbit IgG (Vector) followed by an incubation with ExtrAvidin®-Peroxidase solution (Sigma) and for immunofluorescence by a FITC-conjugated anti-rabbit and Texas Red anti-mouse

antibody (Vector). The peroxidase was visualized with a standard diaminobenzidine/hydrogen reaction for 5 min. For paraffin-embedded human tissue material, sections (5 µm) were mounted on capillary glass slides (DAKO). Sections were microwaved pre-treated in 10 mM citrate buffer pH 6.0 for 15 minutes at 800 W for antigen retrieval. An automated immunostainer (TechMate™ 500 Plus, DAKO) was used for the staining procedure using DAKO ChemMate Kit Peroxidase/3-3´ diaminobenzidine. The indicated primary antibodies were used.

Quantification of microglial population in animal models

Reactive and resident microglial cells were counted in LPS-injected rats and MPTP-exposed mice detected by Iba1 immunohistochemistry based on morphological features. For each animal, eight sections covering the entire antero-posterior ventral mesencephalon were analyzed. For each section, 4 photographs were taken using a 20x magnification (2 for each SN) and microglial cells were counted with the analySIS® software.

Quantification of the striato-nigral dopaminergic system

TH immunohistochemistry in the striatum of mice intoxicated with MPTP was quantified using a computer-assisted software (analySIS®). To carry out the quantification, five striatal sections from each condition, and processed under identical experimental conditions, were scanned at high resolution. The striatal region was delineated and its optical density measured based upon a calibrated grey scale. Quantification of TH-positive cells in the SN was performed according to a modified stereological approach using the Olympus CAST-Grid system. The area of the SN region was estimated using the principle of Cavalieri. All data were collected while blind to experimental treatment and expressed as number of neurons per SN.

Additional Reference

- 51 Li, J. Y. *et al.* Lewy bodies in grafted neurons in subjects with Parkinson's disease suggest host-to-graft disease propagation. *Nat Med* **14**, 501-503 (2008).

Acknowledgments. We thank Drs A. Gorman, O. Hermanson, M. Malewicz, S. Orrenius, T. Panaretakis and B. Zhivotovsky for valuable discussion and Drs L. Hjortsberg, M. Reyland and S. Ceccatelli for providing us with reagents. M. Carballo, J.L. Ribas, A. Fernández and B. Haraldsson provided qualified technical support. This work has been supported by grants from Spanish Ministerio de Ciencia y Tecnología (SAF2006-04119 and 2009-13778), the Swedish Research Council, the Parkinson Foundation of Sweden, the Swedish Alzheimer Foundation and the Swedish Cancer Society. MAB, TD and PB are members of Neurofortis and Bagadilico, both of which are research environments sponsored by the Swedish Research Council.

Author contribution. M.A.B. performed all the experiments except otherwise noted. qPCR was performed by A.G.Q and E.K. J.L.V. and J.C collaborated in doing surgery and further dissecting the animal brains. M.A.B. and T.D. performed primary cell culture experiments and cytokine analysis. E.K. collaborated in performing the caspase activity assay. B.J. and E.K collaborated in performing FACS. B.J. collaborated also in the confocal imaging analysis. E.E. did the neuropathology of the PD, AD and control subjects. A.P. prepared tissue and participated in the morphological assessment of human brain specimens. N.H. and P.B. were involved in study design. M.A.B., J.L.V and B.J. designed the study, analyzed and interpreted the data. All authors discussed the results and commented on or edited the manuscript. The first draft of the paper was written by B.J. J.L.V. and B.J. share senior authorship of the manuscript.

References

- 1 Hanisch, U. K. & Kettenmann, H. Microglia: active sensor and versatile effector cells in the normal and pathologic brain. *Nat Neurosci* **10**, 1387-1394 (2007).

- 2 Block, M. L., Zecca, L. & Hong, J. S. Microglia-mediated neurotoxicity:
uncovering the molecular mechanisms. *Nat Rev Neurosci* **8**, 57-69 (2007).
- 3 Aarli, J. A. Role of cytokines in neurological disorders. *Curr Med Chem* **10**,
1931-1937 (2003).
- 4 Chao, C. C., Hu, S., Molitor, T. W., Shaskan, E. G. & Peterson, P. K.
Activated microglia mediate neuronal cell injury via a nitric oxide
mechanism. *J Immunol* **149**, 2736-2741 (1992).
- 5 Lee, S. J. & Lee, S. Toll-like receptors and inflammation in the CNS. *Curr*
Drug Targets Inflamm Allergy **1**, 181-191 (2002).
- 6 Castano, A., Herrera, A. J., Cano, J. & Machado, A. Lipopolysaccharide
intranigral injection induces inflammatory reaction and damage in
nigrostriatal dopaminergic system. *J Neurochem* **70**, 1584-1592 (1998).
- 7 Saijo, K. *et al.* A Nurr1/CoREST pathway in microglia and astrocytes protects
dopaminergic neurons from inflammation-induced death. *Cell* **137**, 47-59
(2009).
- 8 Zhao, J. *et al.* IRF-8/interferon (IFN) consensus sequence-binding protein is
involved in Toll-like receptor (TLR) signaling and contributes to the cross-
talk between TLR and IFN-gamma signaling pathways. *J Biol Chem* **281**,
10073-10080 (2006).
- 9 Car, B. D. *et al.* Interferon gamma receptor deficient mice are resistant to
endotoxic shock. *J Exp Med* **179**, 1437-1444 (1994).
- 10 Jin, J. J., Kim, H. D., Maxwell, J. A., Li, L. & Fukuchi, K. Toll-like receptor 4-
dependent upregulation of cytokines in a transgenic mouse model of
Alzheimer's disease. *J Neuroinflammation* **5**, 23 (2008).
- 11 Balistreri, C. R. *et al.* Association between the polymorphisms of TLR4 and
CD14 genes and Alzheimer's disease. *Curr Pharm Des* **14**, 2672-2677
(2008).
- 12 Walter, S. *et al.* Role of the toll-like receptor 4 in neuroinflammation in
Alzheimer's disease. *Cell Physiol Biochem* **20**, 947-956 (2007).
- 13 Nicholson, D. W. *et al.* Identification and inhibition of the ICE/CED-3
protease necessary for mammalian apoptosis. *Nature* **376**, 37-43 (1995).
- 14 Cohen, G. M. Caspases: the executioners of apoptosis. *Biochem J* **326 (Pt**
1), 1-16 (1997).
- 15 Keller, M., Ruegg, A., Werner, S. & Beer, H. D. Active caspase-1 is a
regulator of unconventional protein secretion. *Cell* **132**, 818-831 (2008).
- 16 Schulz, J. B. *et al.* Extended therapeutic window for caspase inhibition and
synergy with MK-801 in the treatment of cerebral histotoxic hypoxia. *Cell*
Death Differ **5**, 847-857 (1998).
- 17 Braun, J. S. *et al.* Neuroprotection by a caspase inhibitor in acute bacterial
meningitis. *Nat Med* **5**, 298-302 (1999).
- 18 Cutillas, B., Espejo, M., Gil, J., Ferrer, I. & Ambrosio, S. Caspase inhibition
protects nigral neurons against 6-OHDA-induced retrograde degeneration.
Neuroreport **10**, 2605-2608 (1999).
- 19 Whitton, P. S. Inflammation as a causative factor in the aetiology of
Parkinson's disease. *Br J Pharmacol* **150**, 963-976 (2007).
- 20 Depino, A. M. *et al.* Microglial activation with atypical proinflammatory
cytokine expression in a rat model of Parkinson's disease. *Eur J Neurosci* **18**,
2731-2742 (2003).
- 21 Kawai, T. & Akira, S. Signaling to NF-kappaB by Toll-like receptors. *Trends*
Mol Med **13**, 460-469 (2007).
- 22 Zhang, S. C. & Fedoroff, S. Neuron-microglia interactions in vitro. *Acta*
Neuropathol **91**, 385-395 (1996).
- 23 Gibbons, H. M. & Dragunow, M. Microglia induce neural cell death via a
proximity-dependent mechanism involving nitric oxide. *Brain Res* **1084**, 1-
15 (2006).

- 24 Schumann, R. R. *et al.* Lipopolysaccharide activates caspase-1 (interleukin-1-converting enzyme) in cultured monocytic and endothelial cells. *Blood* **91**, 577-584 (1998).
- 25 Li, P. *et al.* Mice deficient in IL-1 beta-converting enzyme are defective in production of mature IL-1 beta and resistant to endotoxic shock. *Cell* **80**, 401-411 (1995).
- 26 Friedlander, R. M. *et al.* Expression of a dominant negative mutant of interleukin-1 beta converting enzyme in transgenic mice prevents neuronal cell death induced by trophic factor withdrawal and ischemic brain injury. *J Exp Med* **185**, 933-940 (1997).
- 27 Fernandes-Alnemri, T. *et al.* In vitro activation of CPP32 and Mch3 by Mch4, a novel human apoptotic cysteine protease containing two FADD-like domains. *Proc Natl Acad Sci U S A* **93**, 7464-7469 (1996).
- 28 Nunez, G., Benedict, M. A., Hu, Y. & Inohara, N. Caspases: the proteases of the apoptotic pathway. *Oncogene* **17**, 3237-3245 (1998).
- 29 Slee, E. A., Adrain, C. & Martin, S. J. Serial killers: ordering caspase activation events in apoptosis. *Cell Death Differ* **6**, 1067-1074 (1999).
- 30 Aliprantis, A. O., Yang, R. B., Weiss, D. S., Godowski, P. & Zychlinsky, A. The apoptotic signaling pathway activated by Toll-like receptor-2. *Embo J* **19**, 3325-3336 (2000).
- 31 Jung, D. Y. *et al.* TLR4, but not TLR2, signals autoregulatory apoptosis of cultured microglia: a critical role of IFN-beta as a decision maker. *J Immunol* **174**, 6467-6476 (2005).
- 32 Kuno, R. *et al.* Autocrine activation of microglia by tumor necrosis factor-alpha. *J Neuroimmunol* **162**, 89-96 (2005).
- 33 Storz, P., Doppler, H. & Toker, A. Protein kinase Cdelta selectively regulates protein kinase D-dependent activation of NF-kappaB in oxidative stress signaling. *Mol Cell Biol* **24**, 2614-2626 (2004).
- 34 Vancurova, I., Miskolci, V. & Davidson, D. NF-kappa B activation in tumor necrosis factor alpha-stimulated neutrophils is mediated by protein kinase Cdelta. Correlation to nuclear Ikappa Balpha. *J Biol Chem* **276**, 19746-19752 (2001).
- 35 Yoshida, K. PKCdelta signaling: mechanisms of DNA damage response and apoptosis. *Cell Signal* **19**, 892-901 (2007).
- 36 Reyland, M. E., Anderson, S. M., Matassa, A. A., Barzen, K. A. & Quissell, D. O. Protein kinase C delta is essential for etoposide-induced apoptosis in salivary gland acinar cells. *J Biol Chem* **274**, 19115-19123 (1999).
- 37 Czlonkowska, A., Kohutnicka, M., Kurkowska-Jastrzebska, I. & Czlonkowski, A. Microglial reaction in MPTP (1-methyl-4-phenyl-1,2,3,6-tetrahydropyridine) induced Parkinson's disease mice model. *Neurodegeneration* **5**, 137-143 (1996).
- 38 Gonzalez-Scarano, F. & Baltuch, G. Microglia as mediators of inflammatory and degenerative diseases. *Annu Rev Neurosci* **22**, 219-240 (1999).
- 39 Jordan, J., Segura, T., Brea, D., Galindo, M. F. & Castillo, J. Inflammation as therapeutic objective in stroke. *Curr Pharm Des* **14**, 3549-3564 (2008).
- 40 Lenzlinger, P. M., Morganti-Kossmann, M. C., Laurer, H. L. & McIntosh, T. K. The duality of the inflammatory response to traumatic brain injury. *Mol Neurobiol* **24**, 169-181 (2001).
- 41 Allan, S. M. & Rothwell, N. J. Inflammation in central nervous system injury. *Philos Trans R Soc Lond B Biol Sci* **358**, 1669-1677 (2003).
- 42 Karatas, H. *et al.* A nanomedicine transports a peptide caspase-3 inhibitor across the blood-brain barrier and provides neuroprotection. *J Neurosci* **29**, 13761-13769 (2009).
- 43 Bilsland, J. & Harper, S. Caspases and neuroprotection. *Curr Opin Investig Drugs* **3**, 1745-1752 (2002).
- 44 Friedlander, R. M. Apoptosis and caspases in neurodegenerative diseases. *N Engl J Med* **348**, 1365-1375 (2003).

- 45 Le, D. A. *et al.* Caspase activation and neuroprotection in caspase-3-deficient mice after in vivo cerebral ischemia and in vitro oxygen glucose deprivation. *Proc Natl Acad Sci U S A* **99**, 15188-15193 (2002).
- 46 Joseph, B. *et al.* p57(Kip2) cooperates with Nurr1 in developing dopamine cells. *Proc Natl Acad Sci U S A* **100**, 15619-15624. (2003).
- 47 Bocchini, V. *et al.* An immortalized cell line expresses properties of activated microglial cells. *J Neurosci Res* **31**, 616-621 (1992).
- 48 Giulian, D. & Baker, T. J. Characterization of ameboid microglia isolated from developing mammalian brain. *J Neurosci* **6**, 2163-2178 (1986).
- 49 Joseph, B. *et al.* Mitochondrial dysfunction is an essential step for killing of non-small cell lung carcinomas resistant to conventional treatment. *Oncogene* **21**, 65-77. (2002).
- 50 Rite, I., Machado, A., Cano, J. & Venero, J. L. Blood-brain barrier disruption induces in vivo degeneration of nigral dopaminergic neurons. *J Neurochem* **101**, 1567-1582 (2007).

Figure legends

Figure 1 | LPS-induced DEVDase activity regulates microglia activation but not cell death. LPS treatment induces DEVDase activity (**a**) and processing of caspase-3 (**b, e**), which are not associated with cell death, as illustrated by cell survival quantification (**c**), absence of PARP cleavage (**d**), absence of Bid cleavage (**f**) and integrity of mitochondrial transmembrane potential as demonstrated by TMRE staining (**g**) in cultured BV2 microglia cells. Caspase-3/7 inhibition by DEVD-fmk (**a**) prevents LPS-induced morphological microglia activation, which is characterized by a bushy appearance with swollen cell bodies and thickened, branched processes (**h, i**) and induction of typical inflammation-related molecules like iNOS (**j, k**) and IKK β (**j, l**) and ROS formation (**m**). STS: staurosporine is used as an apoptosis inducer. Data are expressed as mean \pm SEM (n=3). G3PDH and actin are used as standard for equal loading of protein. Statistical difference was measured by one-way Analysis of variance ANOVA followed by Bonferroni test. #, * p<0.05.

Figure 2 | Knockdown of caspase-3 or caspase-7 decreases microglia activation in response to LPS. Specific siRNAs targeting caspase-3 and/or caspase-7 prevents LPS-induced increase of iNOS expression (**a, b**) in cultured BV2 microglia cells. In addition, caspase-3 or caspase-7 silencing prevents LPS-induced

activation of NF- κ B as seen by reduction of p65 nuclear translocation (**c, d**). Since microglia activation may be deleterious to neuronal cells, we co-cultured neuronal MN9D and microglial BV2 cells. Under these conditions, LPS treatment induces neuronal cell death and caspase-3/7 knockdown in microglia cells prevents neuronal cell death (**e, f**). Caspase 3 or caspase 7 inhibition by DEVD-fmk or IETD-fmk treatment modulates LPS-induced cytokine expression at 12 and 24h in primary microglia cell culture (**g**). Data are expressed as mean \pm SEM (n=3) and \pm SD (n=4) in g. Actin is used as standard for equal loading of protein. Statistical difference was measured by one-way Analysis of variance ANOVA followed by Bonferroni test. ζ , #, * p<0.05. In panel g, ### denotes statistical significant difference between LPS and LPS-DEVD-fmk/IETD-fmk (P<0.001, two way ANOVA, Bonferroni/Dunn) concerning time and treatment.

Figure 3 | Caspase-8 activity controls LPS-induced caspase-3/7 activation.

Caspase-8 inhibition by IETD-fmk, but not caspase-1 inhibition by YVAD-fmk prevents LPS-induced DEVDase activity (**a**). LPS treatment induces caspase-8 (IETDase) activity, which is inhibited by the caspase-8 inhibitor IETD-fmk (**b**) or specific siRNA targeting caspase-8 (**c**) in BV2 cells. Treatment with Fas ligand was used as positive control for IETDase activity induction (**b**). Caspase-8 knockdown using siRNA prevents LPS-induced DEVDase activity (**d**). The use of IETD-fmk or DEVD-fmk has similar inhibitory effects on LPS-induced iNOS expression (**e, f**). Combined treatment with DEVD-fmk and YVAD-fmk possess an additive inhibitory effect over LPS-induced iNOS expression (**e, f**). siRNA knockdown of caspase-8 prevents LPS-induced expression of iNOS (**g, h**). Data are expressed as mean \pm SEM (n=3). Actin is used as standard for equal loading of protein. Statistical difference was measured by one-way Analysis of variance ANOVA followed by Bonferroni test. #,* p<0.05.

Figure 4 | Caspase-3/7 regulates microglia activation via PKC δ pathway.

Immunoblot showing a successful overexpression of PKC δ (**a**). Caspase-3/7 inhibition by DEVD-fmk prevents LPS-induced PKC δ cleavage/ activation in BV2 microglia cells (**b, c**). This data is confirmed by siRNA knockdown of caspase-3 or caspase-7 expression (**d, e**). In addition, PKC δ inhibition by rottlerin mostly abolishes LPS-induced activation of iNOS (**f, g**). Overexpression of PKC δ D327A, a caspase uncleavable PKC δ mutant, has an inhibitory effect on LPS-induced iNOS expression (**h, i**). Rottlerin treatment reduces LPS-induced cytokine expression at 12 and 24h in primary microglia cell culture (**j**). Data are expressed as mean \pm SEM (n=3) and \pm SD (n=4) in i. G3PDH and actin are used as standard for equal loading of protein. Statistical difference was measured by one-way Analysis of variance ANOVA followed by Bonferroni test. *p<0.05. In panel i, ### denotes statistical significant difference between LPS and LPS Rottlerin P<0.001, two way ANOVA, Bonferroni/Dunn) concerning time and treatment.

Figure 5 | *In vivo* inhibition of the caspase dependent pathways prevents microglia activation.

In vivo injection of LPS in rat substantia nigra (insert in panel **a**) induced activation of caspase-8 and caspase-3 in the ventral mesencephalon, which is mostly localized in OX-6-labelled reactive microglia (**b, c**) compared to control (**a**). There is a null coincidence between Hoechst labeled nuclei and caspase8/cleaved caspase 3 immunoreactivity in OX-6-labelled microglia (**b, c**). *In vivo* DEVD-fmk significantly reduced intranigral LPS-induced microglia activation as evaluated by Iba 1 immunohistochemistry (reduction of activated microglia population by 31% at the injection site and 53% at the non-injection site) (**d, e**) and mRNA levels of proinflammatory molecules (**f**). *In vivo* inhibition of caspase-8, caspase-3/7 or PKC δ , using IETD-fmk, DEVD-fmk and Rottlerin respectively, predominantly abolished the intranigral induction of iNOS upon LPS treatment (**g, h**). *In vivo* acute intraperitoneally injections of MPTP in mice highly increased the density of reactive microglia in substantia nigra (+245% increase in

sham group) (**i, j**) Intranigral caspase 8 inhibition by IETD-fmk injections robustly prevented the MPTP-induced microglia activation at the non-injection site (+74% increase in sham group). With respect to the density of the resident microglia at the non-injection site, again, IETD-fmk injection also significantly prevented the MPTP-induced decrease of the resident microglia density (**i, j**). Data are expressed as mean \pm SEM (n=3). Actin is used as standard for equal loading of protein. SNr: Substantia nigra pars reticulata; SNc: Substantia nigra pars compacta. Scale bar: a-c, 25 μ m; d, 500 μ m for low magnification photographs; j, 400 and 100 μ m for low and high-magnification photographs. Statistical difference was measured by one-way Analysis of variance ANOVA followed by Bonferroni test. * p<0.05.

Figure 6 | Activation of caspase-3 and caspase-8 in microglia in brain from Parkinson's and Alzheimer's disease subjects. Double immunolabeling and confocal imaging analysis show significant activation of caspase-8 and caspase-3, which is mostly localized in CD68-labelled microglia, in the ventral mesencephalon in paraffin sections from Parkinson's disease (PD) patients as compared to age- and gender-matched healthy control cases (**a-b**). Confocal images of immunostaining with cleaved caspase-3 (**a**) or cleaved caspase-8 (**b**) (green), together with CD68 (red) antibodies and merge from a control and a PD case are depicted. Similar results were found in the frontal cortex of Alzheimer's disease (AD) patients as compared to age- and gender-matched healthy control cases (**c-d**). Confocal images of immunostaining with cleaved caspase-3 (**c**) or cleaved caspase-8 (**d**) (red), together with CD68 (green) antibodies are depicted. Nuclei were counterstained with Hoechst. Merge from a control and an AD case illustrates the absence of cleaved caspase 3/caspase staining in Hoechst-labelled nuclei in reactive microglia (**c-d**). Scheme illustrating potential pathways of how caspase-8 and caspase-3/7 modulate the inflammatory response in microglia are depicted in panel (**e**). Scale bar 10 μ m.

Supplementary data

Figure S1 | DEVDase activity in response to LPS treatment persists at 24 and 48 hours in BV2 microglia cells (**a, b**). LPS-induced DEVDase activity is not associated with BV2 cell death up to 24 hours as shown by cell survival assay (**c**). The caspase-3/7 inhibitor, DEVD-fmk, does not prevent BV2 cell death occurring at 48 hours post LPS treatment (**d**). DEVDase activity in response to LPS treatment is time- (**e**) and dose-dependent (**f**) in BV2 microglia cells. Data are expressed as mean \pm SEM (n=3). Statistical difference was measured by one-way Analysis of variance ANOVA followed by Bonferroni test.* $p < 0.05$.

Figure S2 | LTA, PamC3sk4, and IFN γ treatment induce DEVDase activity (**a**), which are not associated with cell death as illustrated by cell survival quantification (**b**) and FACS analysis of sub G1 peak appearance (**c**) in cultured BV2 microglia cells. Data are expressed as mean \pm SEM (n=3). Statistical difference was measured by one-way Analysis of variance ANOVA followed by Bonferroni test.* $p < 0.05$.

Figure S3 | LPS-induced DEVDase activity is not associated with BV2 cell death up to 24 hours as shown by scoring of condensed or fragmented nuclei upon nuclear Hoechst staining (**a-d**), or FACS analysis of sub G1 peak appearance (**e-g**). The caspase-3/7 inhibitor, DEVD-fmk does not prevent BV2 cell death occurring at 48 hours post LPS treatment (**d, g**). Data are expressed as mean \pm SEM (n=3). Statistical difference was measured by one-way Analysis of variance ANOVA followed by Bonferroni test.* $p < 0.05$.

Figure S4 | LPS-induced caspase-3 activation in BV2 microglia cells is restricted to the plasma membrane in contrast to staurosporine (STS) treatment, which shows abundant cytoplasmic and nuclear localization (**a-c**). Nuclear and plasma

membrane compartments were labelled with DAPI and Alexa Fluor 555 cholera toxin subunit B conjugates (CTB) respectively. Panel **d** shows quantification, using the LSM module Zeiss Software (for further information visit <http://www.zeiss.de>), of cleaved caspase 3 immunostaining intensity following LPS and staurosporine treatment in BV2 cells. Scale bar 10 μ m.

Figure S5 | Caspase-3/7 inhibition by DEVD-fmk prevents LTA, Pam3CSk4 (**a**) and IFN γ (**b**) -induced iNOS expression in BV2 microglia cells. Caspase-3/7 and caspase-8 inhibition by DEVD-fmk and IETD-fmk respectively prevents Pam3CSk4(**c**), LTA (**d**) and IFN γ (**e**) induced ROS formation in BV2 microglia cells. Data are expressed as mean \pm SEM (n=3). Actin is used as standard for equal loading of protein. Statistical difference was measured by one-way Analysis of variance ANOVA followed by Bonferroni test. #,* p<0.05.

Figure S6 | Specific siRNAs targeting caspase-3 (**a, b**) and/or caspase-7 expression (**c, d**) inhibit DEVDase activity (**e**). siRNA knockdown of caspase-3 or caspase-7 prevents LPS-induced expression of IKK β (**f**) and ROS formation (**g**). LPS-induced IL-1 β , TNF- α and mKC (**h**) and iNOS expression (**i**) are lowered after caspase-3, caspase-7 or caspase-8 knockdown by siRNAs in BV2 microglia cells. Data are expressed as mean \pm SEM (n=3). Actin is used as standard for equal loading of protein. G3PDG is used as standard for equal loading of mRNA. Statistical difference was measured by one-way Analysis of variance ANOVA followed by Bonferroni test. #,* p<0.05.

Figure S7 | Specific siRNAs targeting caspase-3, caspase-7 or caspase-8 expression prevents PamC3sk4 (**a, b, e**), LTA (**c, d, f**), and IFN γ (**g, h, i**)-induced expression of iNOS (**a-d, g, h**) and ROS formation (**e, f, i**) in BV2 microglia cells. Data are expressed as mean \pm SEM (n=3). Actin is used as standard for equal

loading of protein. Statistical difference was measured by one-way Analysis of variance ANOVA followed by Bonferroni test. #,* p<0.05. **(a, b)**

Figure S8 | Chemical or knockdown inhibition of caspase-8 using IETD-fmk **(a)** or siRNA targeting caspase-8 **(b)** respectively prevents LPS-induced ROS formation in BV2 microglia cells. Data are expressed as mean \pm SEM (n=3). Statistical difference was measured by one-way Analysis of variance ANOVA followed by Bonferroni test. #,* p<0.05. **(a, b)**

Figure S9 | LPS exposure of BV2 cells does not lead to processing of the potential caspase-8 substrates HDAC7 and RIP1. Data are expressed as mean \pm SEM (n=3). G3PDH is used as standard for equal loading of protein. Statistical difference was measured by one-way Analysis of variance ANOVA followed by Bonferroni test.

Figure S10 | LPS treatment fails to induce VEIDase activity **(a)** and chemical inhibition of caspase-6 using VEID-fmk **(b)** does not affect LPS-induced DEVDase activity in BV2 microglia cells. Statistical difference was measured by one-way Analysis of variance ANOVA followed by Bonferroni test. * p<0.05. **(a, b)**

Figure S11 | Caspase-3 and -8 processing/activation is dependant on TLR4 but independent of MyD88. Specific siRNAs targeting TLR4 **(a)** inhibit LPS-induced caspase-8 cleavage **(b)** and caspase-3 cleavage **(c)** as measured by FACS analysis in BV2 cells. Specific siRNAs targeting MyD88 **(d)** do not inhibit LPS-induced caspase-8 cleavage **(e)** and caspase-3 cleavage **(f)** in BV2 cells. G3PDH is used as standard for equal loading of protein and mRNA. Data are expressed as mean \pm SEM (n=3). Statistical difference was measured by Kolmogorov–Smirnov test (K-S statistics) for FACS analysis and one-way Analysis of variance ANOVA followed by Bonferroni test. #,* p<0.05.

Figure S12 | Panels **a-d** show quantification, using FACS analysis, of cleaved caspase-3 and 8 following exposure of LPS and/or TNF α R1 neutralizing antibodies to BV2 cells. The values presented in b and d show how inhibition of TNF α signaling fail to alter the LPS-induced cleavage of caspase-3 and 8 6h after toxin challenge. Panel **e** shows a decrease in LPS-induced iNOS expression after 24h of treatment with TNF α R1 ab. Data are expressed as mean \pm SEM (n=3). Statistical difference was measured by Kolmogorov–Smirnov test (K-S statistics) for FACS analysis and one-way Analysis of variance ANOVA followed by Bonferroni test. #,* p<0.05.

Figure S13 | PKC δ overexpression enhances LPS-induced iNOS expression and this effect requires DEVDase activity as it is inhibited by DEVD-fmk treatment. Actin is used as standard for equal loading of protein. Data are expressed as mean \pm SEM (n=3). Statistical difference was measured by one-way Analysis of variance ANOVA followed by Bonferroni test. * p<0.05.

Figure S14 | Intranigral vehicle injections containing 1% DMSO highly induce the density of reactive microglia in sham and MPTP-intoxicated mice, while IETD-fmk strongly prevents this effect. Panel a shows low and high-magnification photographs of Iba1 immunohistochemistry at the injection site in the ventral mesencephalon of sham, MPTP and MTP-IETD-fmk groups. Panel b shows quantification of activated and resident microglia cell density for each experimental group. Panel c shows TH immunohistochemistry in the striatum (upper panel) and the ventral mesencephalon (lower panel) of sham, MPTP and MTP-IETD-fmk groups. Panel d shows densitometric quantitation of striatal dopaminergic density and panel e stereological nigral TH cell counts demonstrating a modest but yet significant protective effect of IETD-fmk against the neurotoxic effect of MPTP. Scale bar: a, 400 and 100 μ m for low and high-magnification photographs; c, 950 and 400 μ m for upper and lower panel respectively. Statistical difference was measured by one-way Analysis of variance ANOVA followed by Bonferroni test

Figure S15 | Analysis of cleaved caspase-3 staining pattern in paraffin-embedded mesencephalic tissue sections covering the substantia nigra from PD subjects as compared to matched healthy control case. Notice the weak cytoplasmic staining of cleaved caspase-3 in the SN of PD cases compared to control case. Microglial cells were stained with CD68 antibody to determinate activation (data not shown). As a positive control for cleaved caspase-3, sections of colonic mucosa were stained, according to the manufacture's instructions.

Figure S16 | Analysis of cleaved caspase-8 staining pattern in paraffin-embedded mesencephalic tissue sections covering the substantia nigra from PD subjects as compared to matched healthy control case. Robust cleaved caspase-8 staining was more obviously localized in the cell cytoplasm in the SN of PD cases compared to control case. As a positive control for cleaved caspase-8, sections of colonic mucosa were stained, according to the producer's instructions.

Figure S17 | Analysis of cleaved caspase-3 staining pattern in paraffin-embedded of frontal cortex from AD subjects as compared to matched healthy control case. Notice the weak cytoplasmic staining of cleaved caspase-3 in the frontal cortex of AD cases compared to control case. As a positive control for cleaved caspase-3, sections of colonic mucosa were used also here.

Figure S18 | Analysis of cleaved caspase-8 staining pattern in frontal cortex from AD subjects as compared to matched healthy control case. Robust cleaved caspase-8 staining was more obviously localized in the cell cytoplasm in the frontal cortex of PD cases compared to control case. As a positive control for cleaved caspase-8, sections of colonic mucosa were stained, according to the producer's instructions.

Figure S19 | Colocalization analysis of cleaved caspase-3 (**a**) or cleaved caspase-8 (**b**) and CD68 microglia staining pattern marker in control and PD substantia nigra's patients using the Zeiss Software (colocalized pixels are pseudocolored white; for further information visit <http://www.zeiss.de>). This analysis demonstrates that most active caspase-3 and caspase-8 immunoreactivity in the ventral mesencephalon of PD patients is localized within CD68-labelled microglia.

Movie S1 | LPS-induced caspase-3 activation in BV2 microglia cells is restricted to plasma membrane compartment. Confocal analysis of active caspase-3 subcellular localization was performed by immunofluorescence using an anti-cleaved caspase-3 (Asp175) antibody revealed by an Alexa Fluor 488-conjugated secondary antibody (green). Nuclear and plasma membrane compartments were labelled with DAPI (Blue) and Alexa Fluor 555 cholera toxin subunit B conjugates (CTB, red) respectively. 3D reconstruction of serial z stack confocal images is presented.

Movie S2 | STS-induced caspase-3 activation in BV2 microglia cells accumulates in the nuclear compartment. Confocal analysis of active caspase-3 subcellular localization was performed by immunofluorescence using an anti-cleaved caspase-3 (Asp175) antibody revealed by an Alexa Fluor 488-conjugated secondary antibody (green). Nuclear and plasma membrane compartments were labelled with DAPI (Blue) and Alexa Fluor 555 cholera toxin subunit B conjugates (CTB, red) respectively. 3D reconstruction of serial z stack confocal images is presented.

Table S1 | Antibodies and blocking peptides used in this study.

Table S2 | PCR primers used in this study. All primer sets had similar T_m values and amplified short fragments, spanning an intron and recognizing all cDNA splicing variants described.

Table S3 | ON-TARGETplus SMART pool small interfering RNAs used in this study.

This technology is based on the use of four duplex siRNA's targeting four different regions of the mRNA to be targeted (SMARTpool). This technology is also based on dual-strand modification (ON-TARGETplus) proven to reduce off target effects caused by both strands.

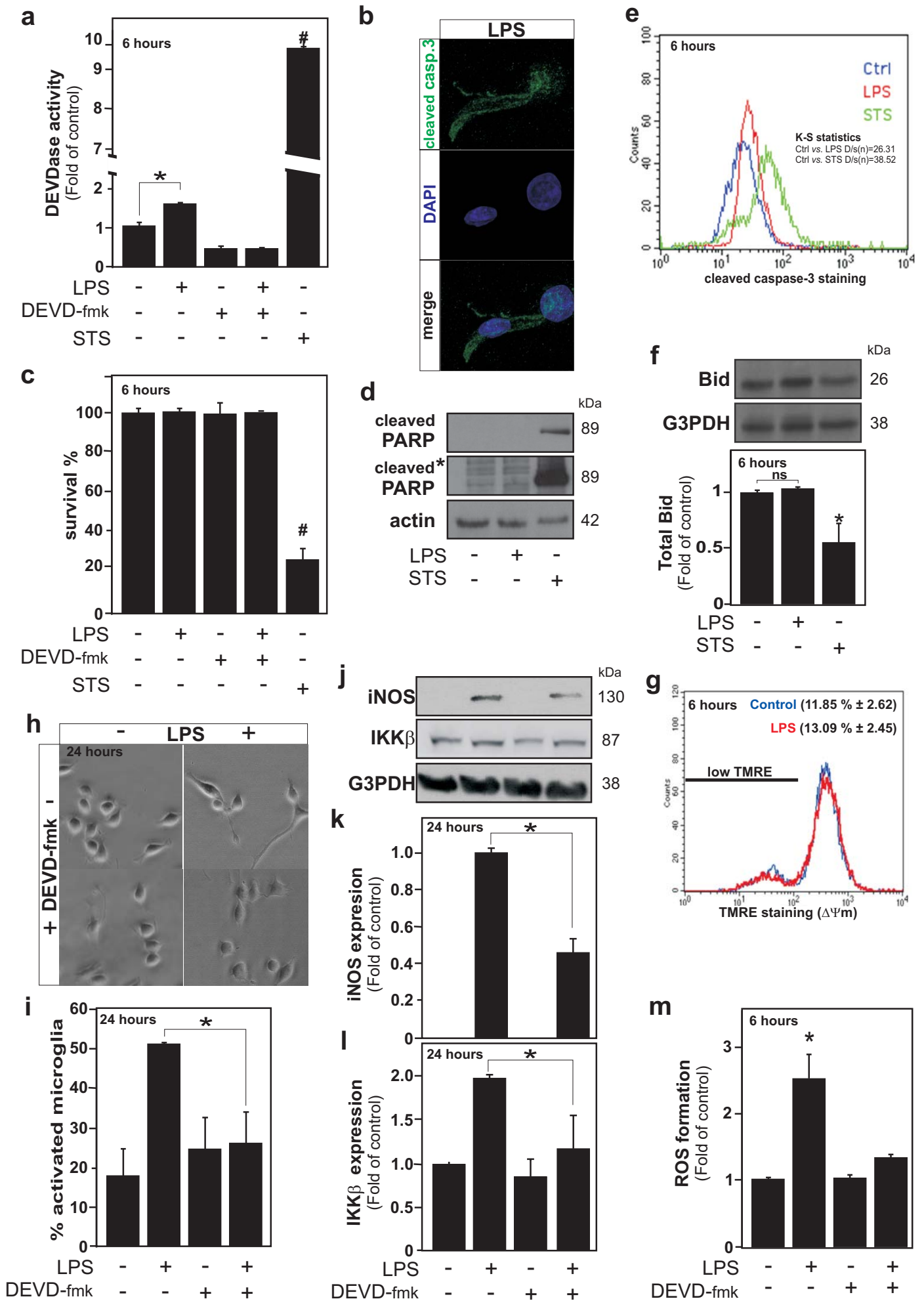


Fig 1. Burguillos et al

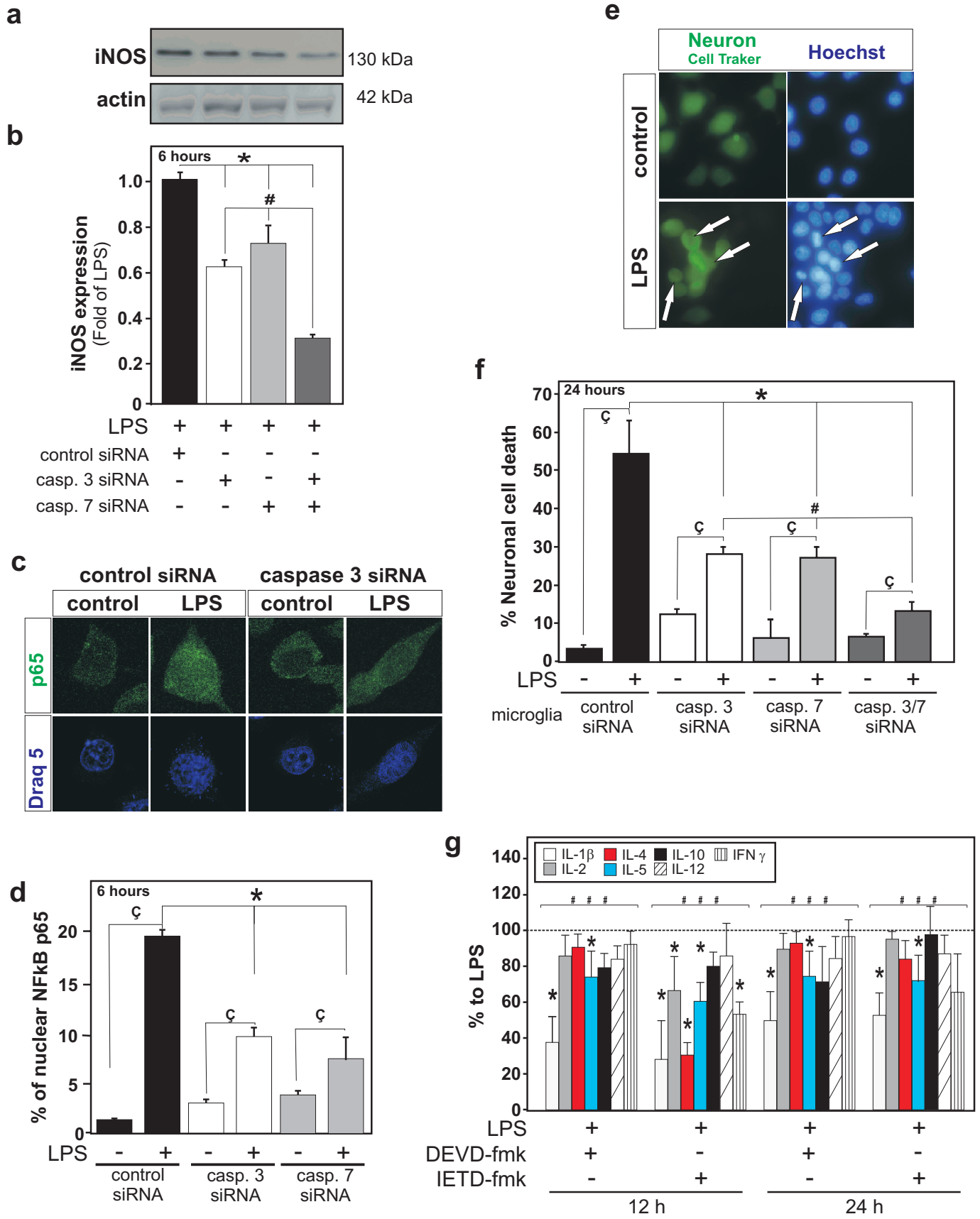


Fig 2. Burguillos et al

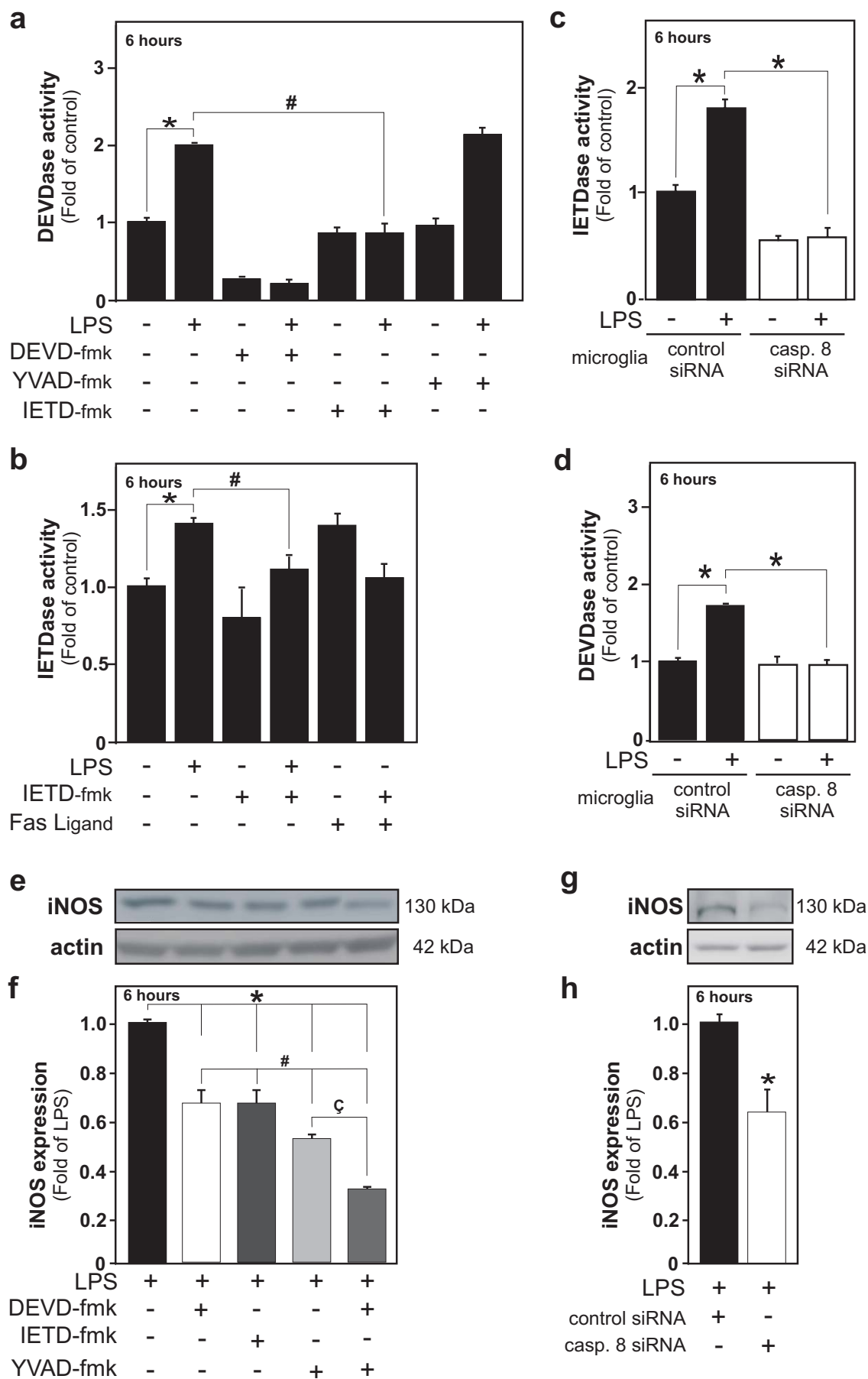


Fig 3. Burguillos et al

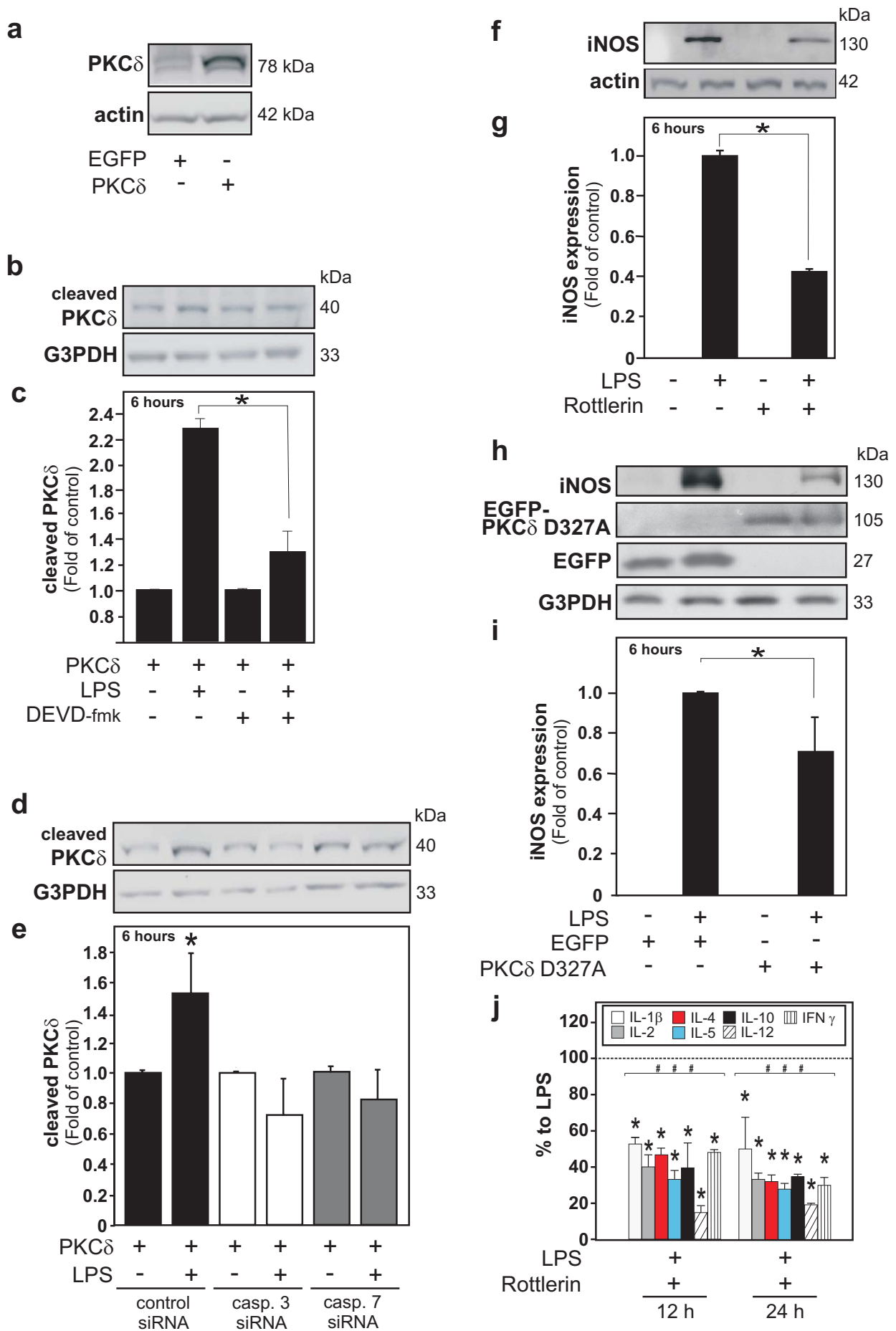


Fig 4. Burguillos et al

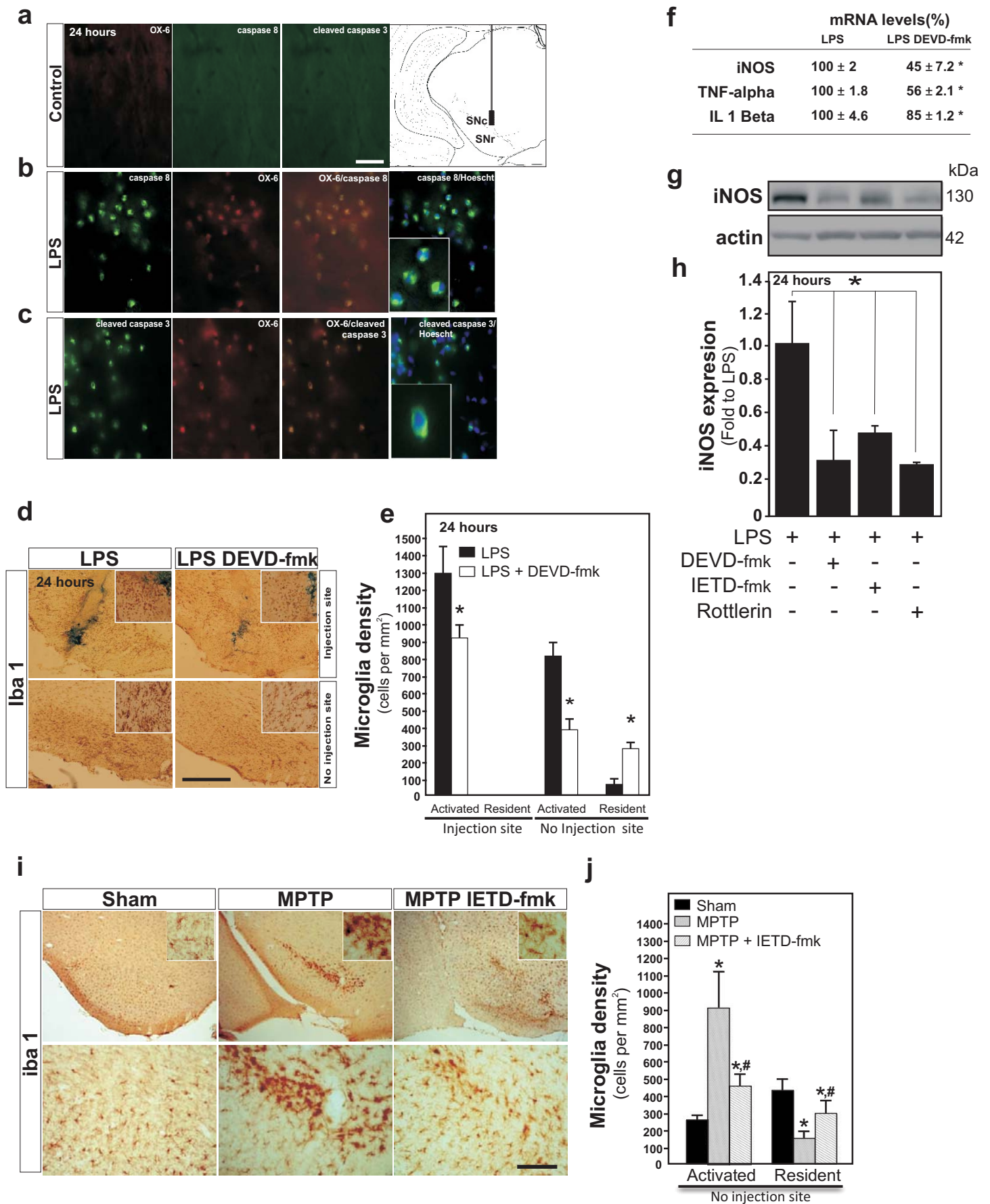


Fig 5. Burguillos et al

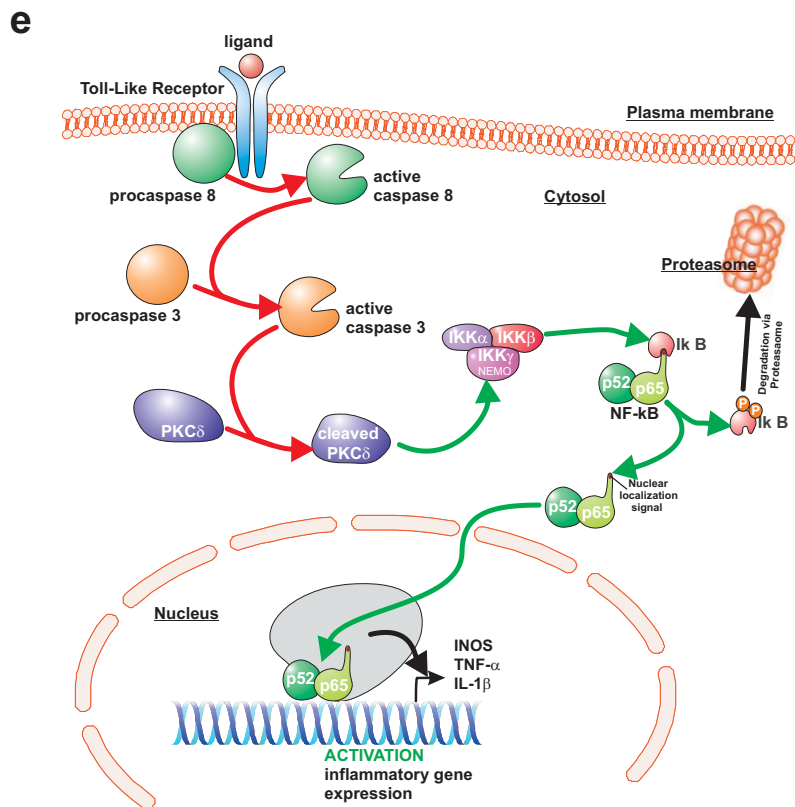
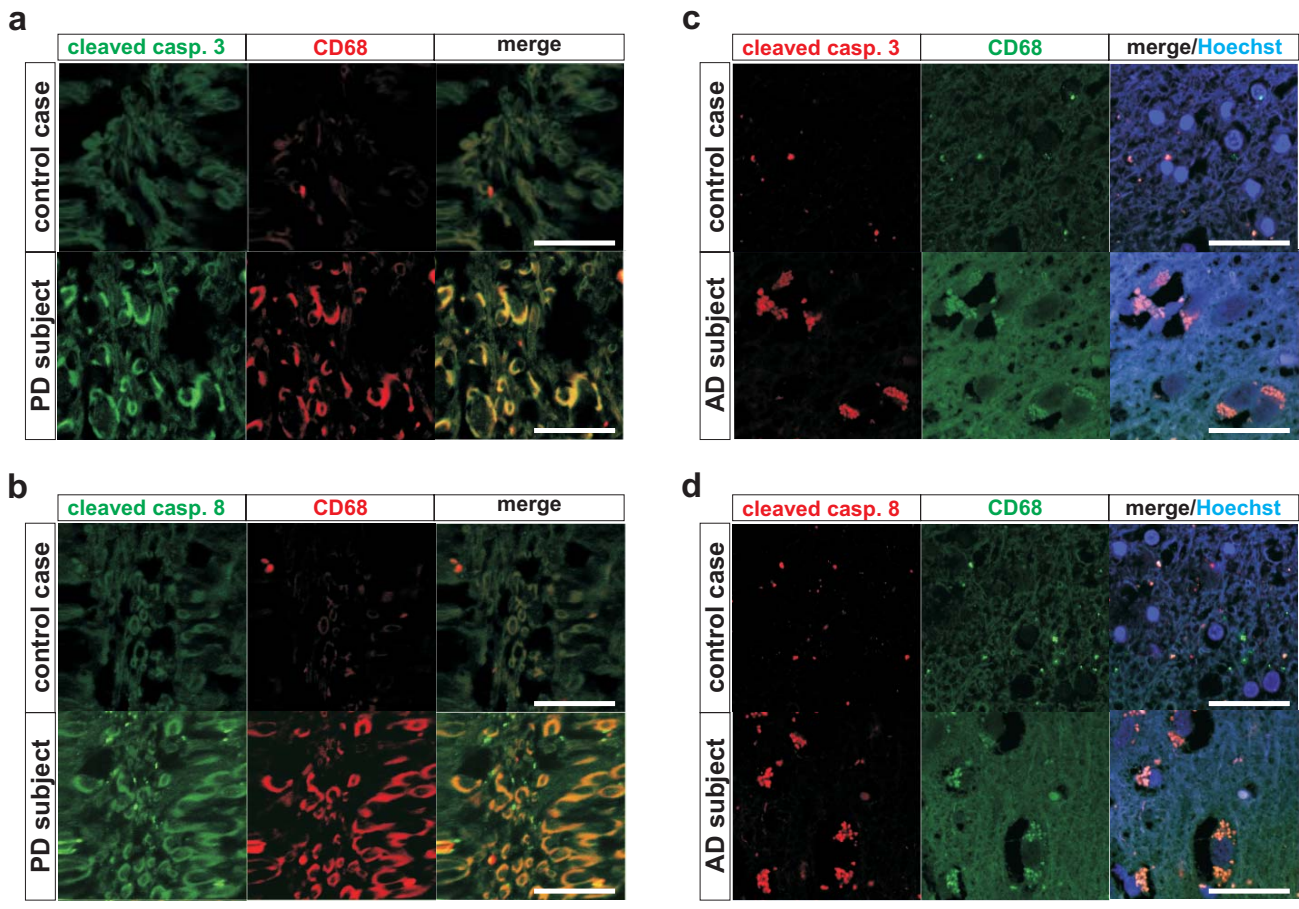


Fig 6. Burguillos et al

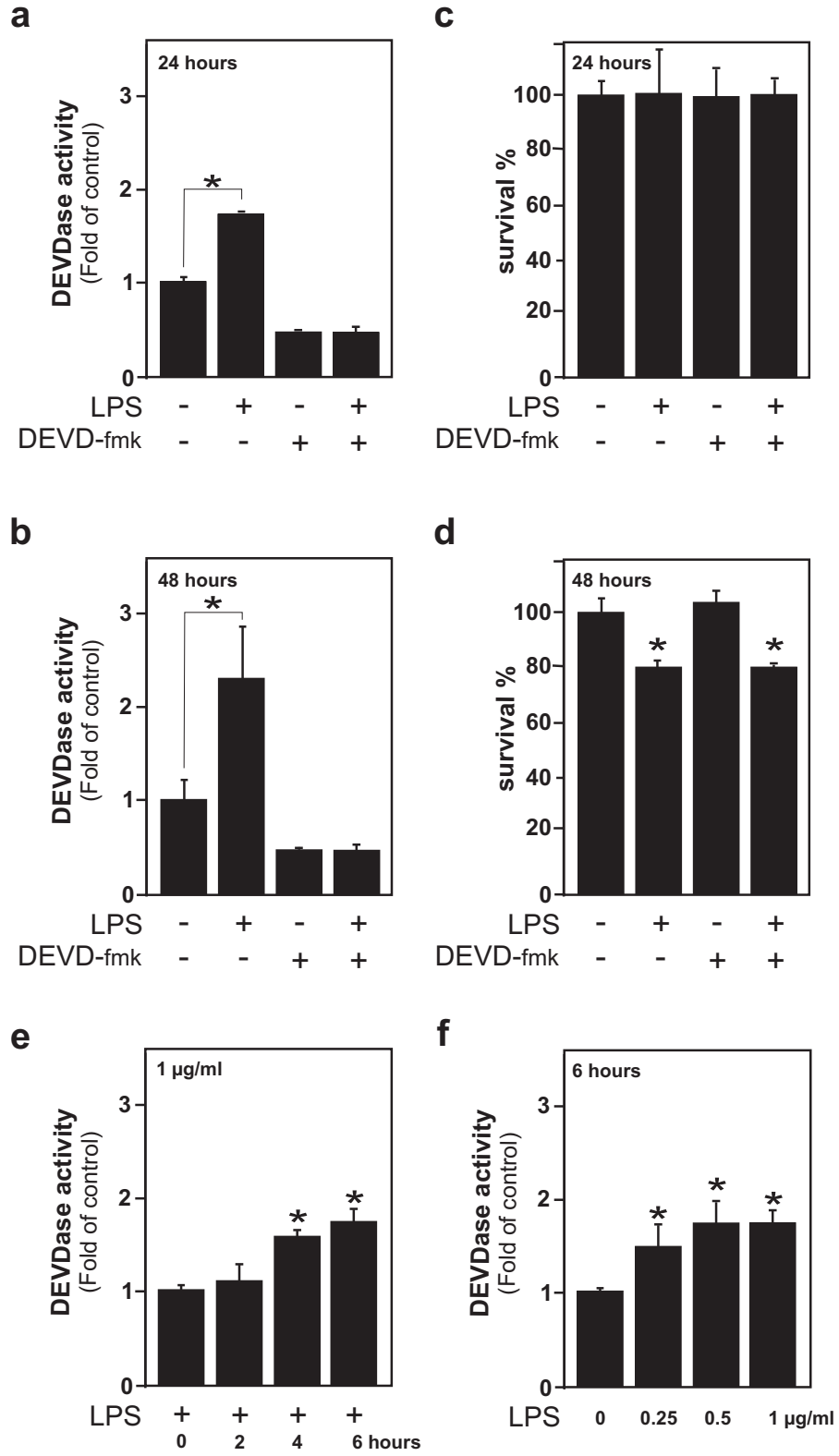


Fig S1. Burguillos et al

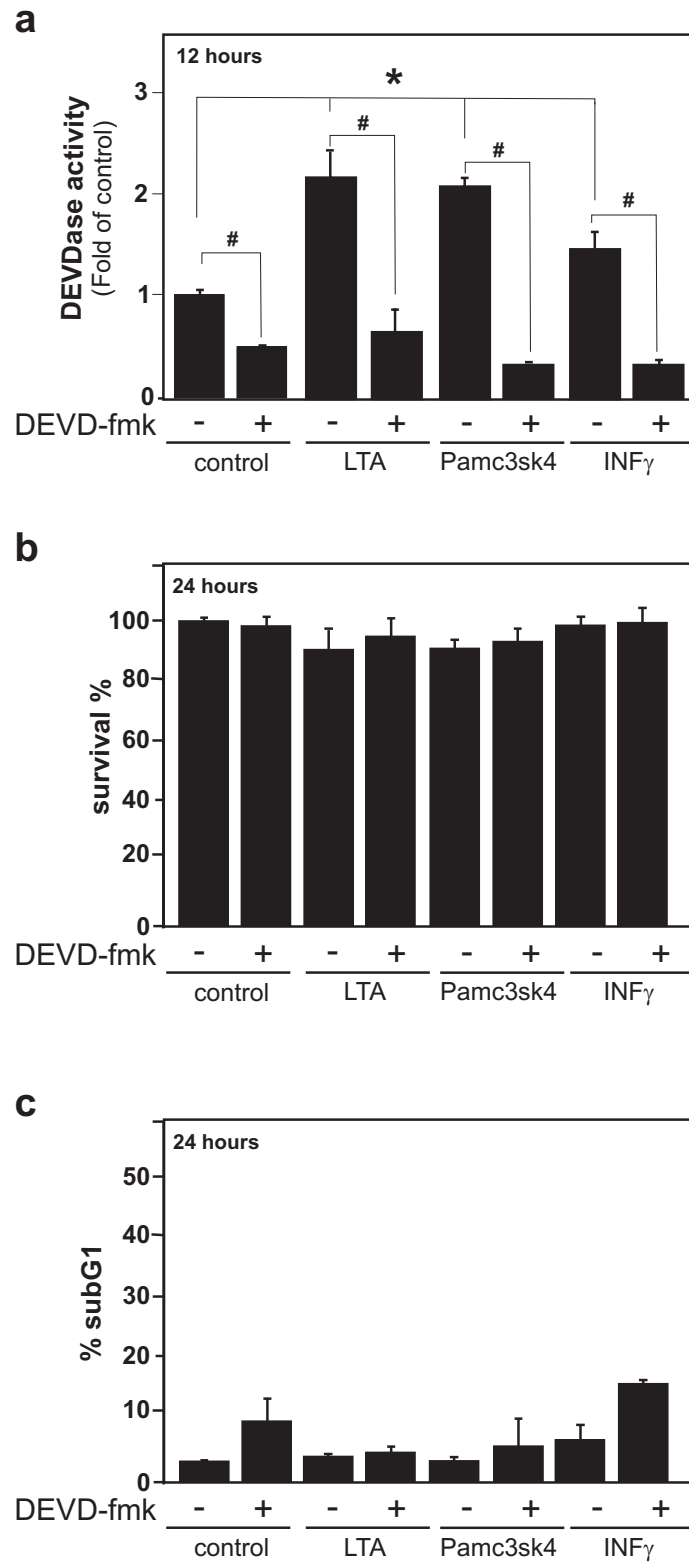


Fig S2. Burguillos et al

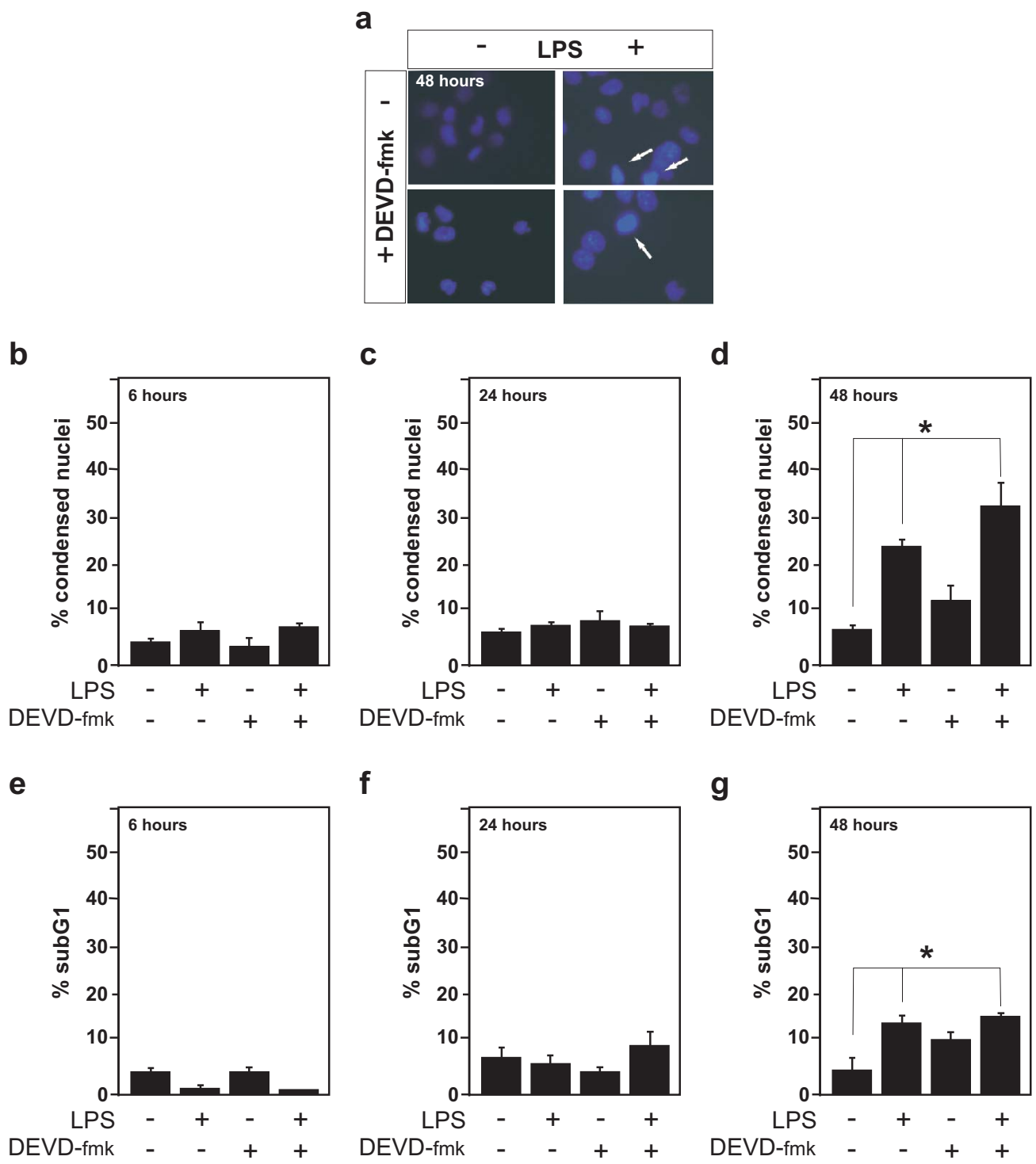


Fig S3. Burguillos et al

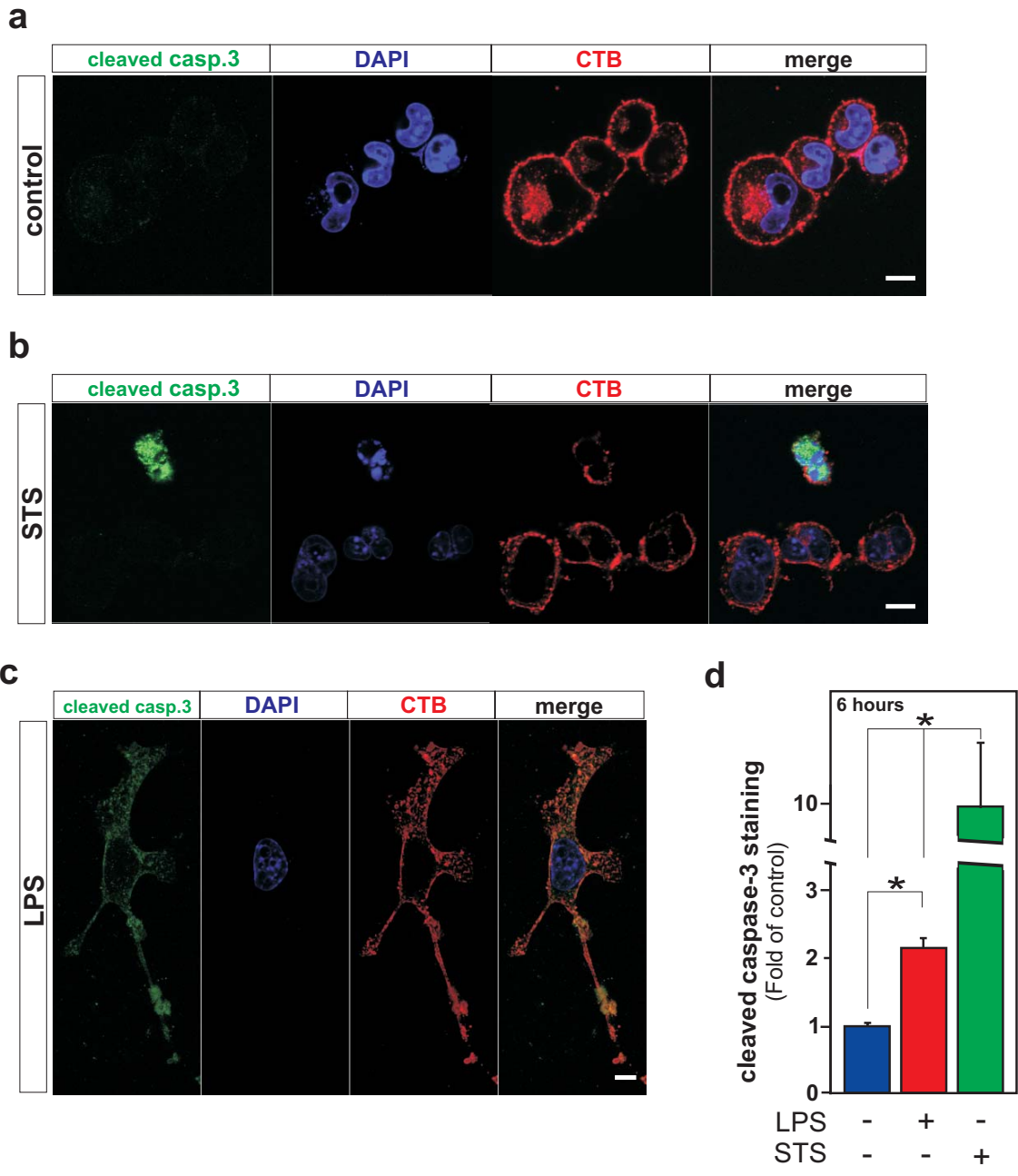


Fig S4. Burguillos et al

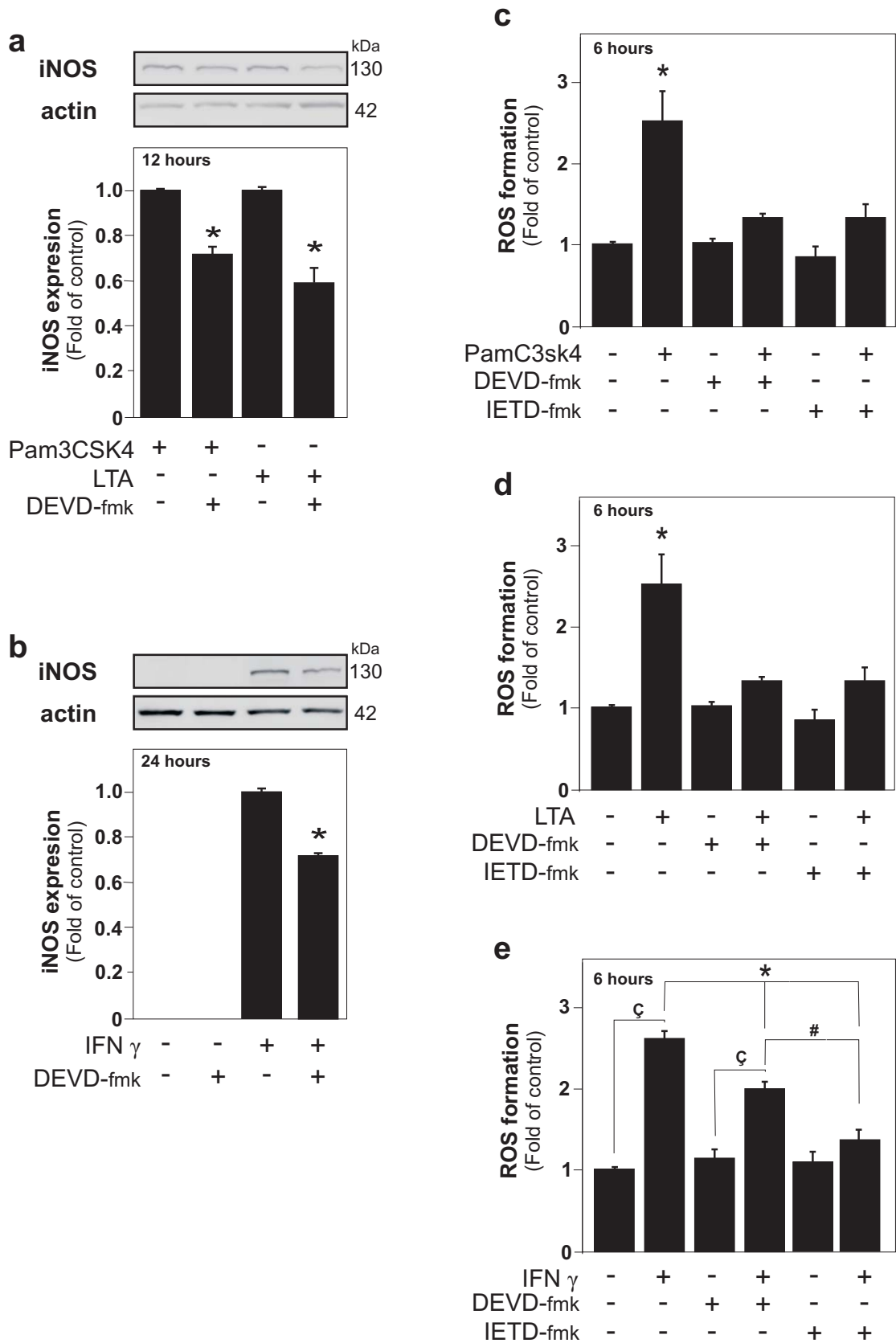


Fig S5. Burguillos et al

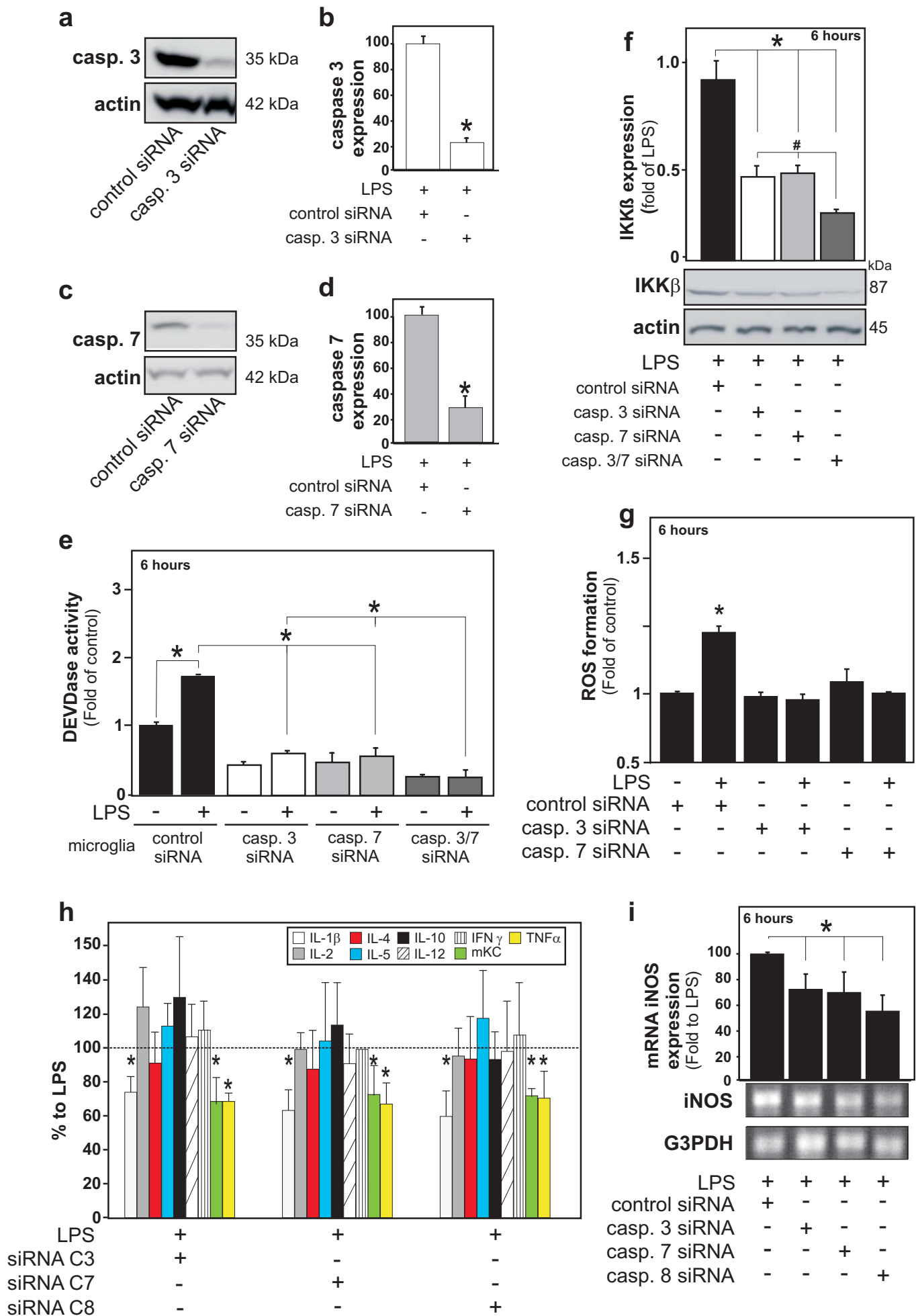
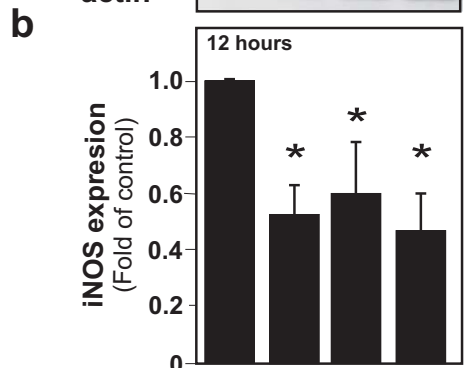
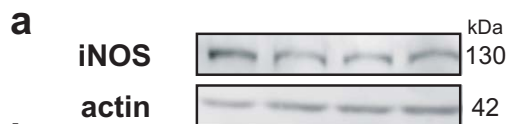
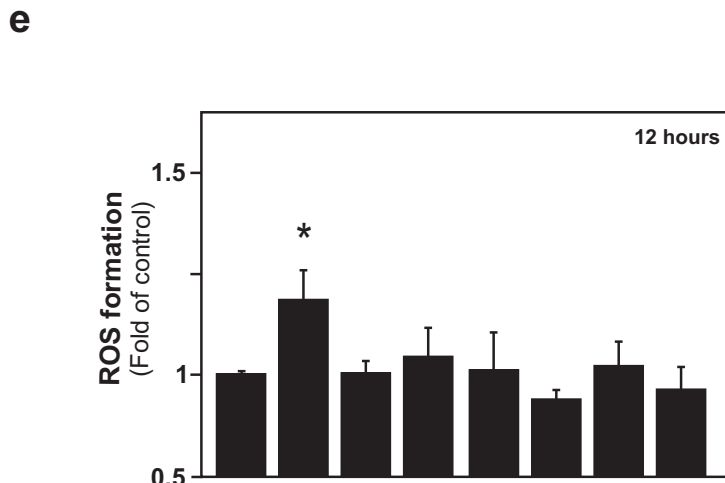


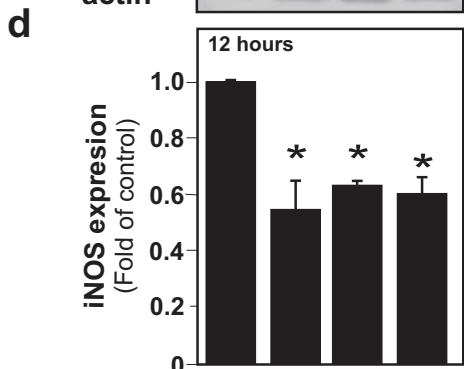
Fig S6. Burguillos et al



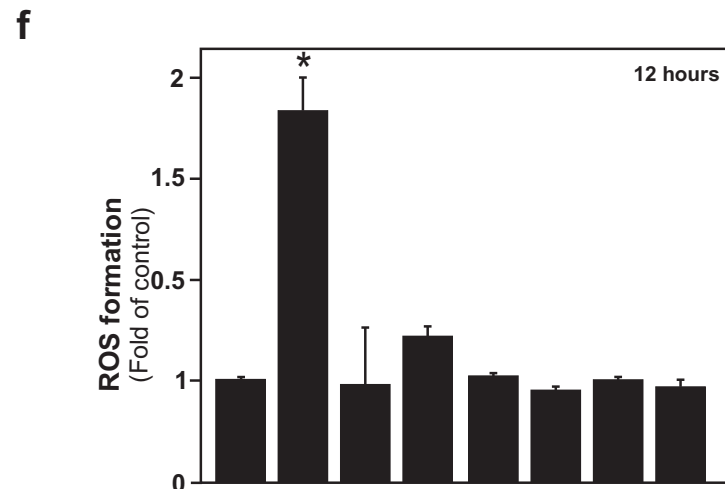
PamC3sk4	+	+	+	+
Control siRNA	+	-	-	-
Casp. 3 siRNA	-	+	-	-
Casp. 7 siRNA	-	-	+	-
Casp. 8 siRNA	-	-	-	+



PamC3sk4	-	+	-	+	-	+	-	+
Control siRNA	+	+	-	-	-	-	-	-
Casp. 3 siRNA	-	-	+	+	-	-	-	-
Casp. 7 siRNA	-	-	-	-	+	+	-	-
Casp. 8 siRNA	-	-	-	-	-	-	+	+



LTA	+	+	+	+
Control siRNA	+	-	-	-
Casp. 3 siRNA	-	+	-	-
Casp. 7 siRNA	-	-	+	-
Casp. 8 siRNA	-	-	-	+



LTA	-	+	-	+	-	+	-	+
Control siRNA	+	+	-	-	-	-	-	-
Casp. 3 siRNA	-	-	+	+	-	-	-	-
Casp. 7 siRNA	-	-	-	-	+	+	-	-
Casp. 8 siRNA	-	-	-	-	-	-	+	+

Fig S7. Burguillos et al

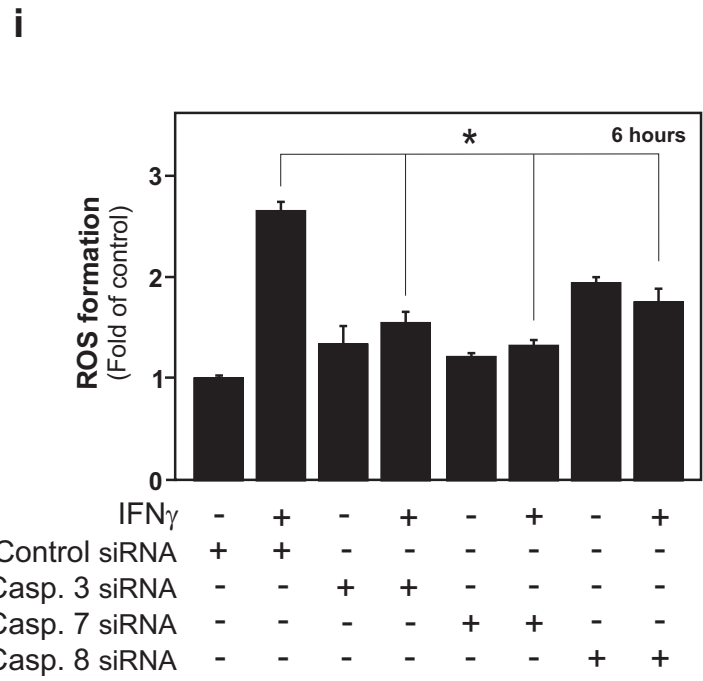
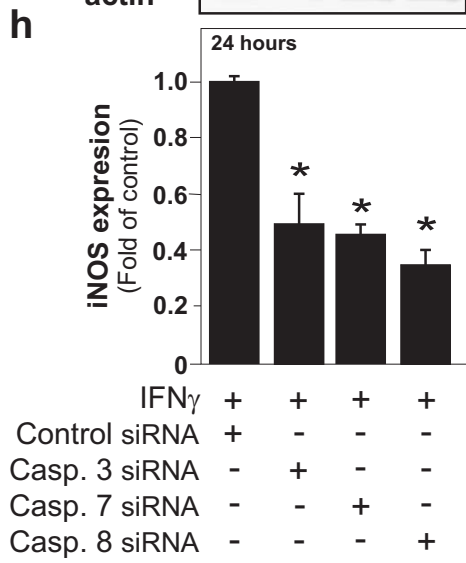
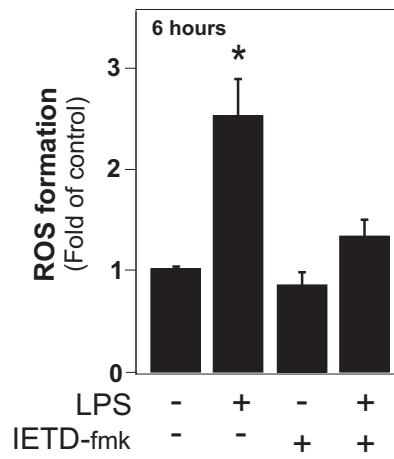


Fig S7 (continued). Burguillos et al

a



b

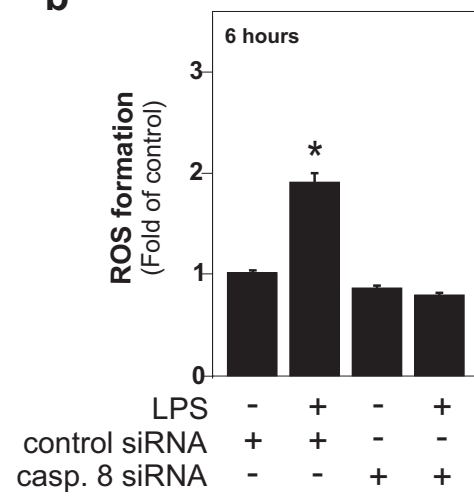


Fig S8. Burguillos et al

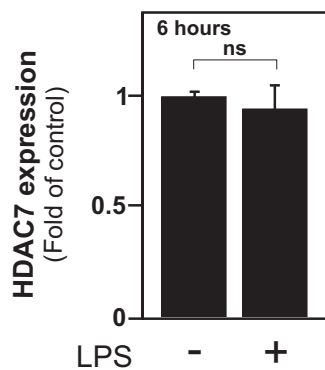
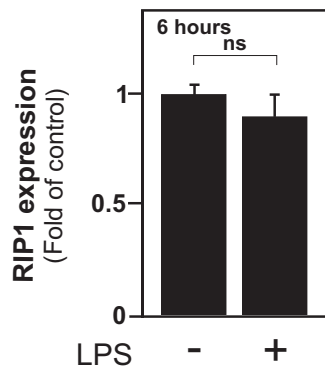
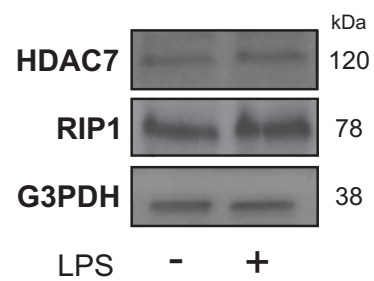


Fig S9. Burguillos et al

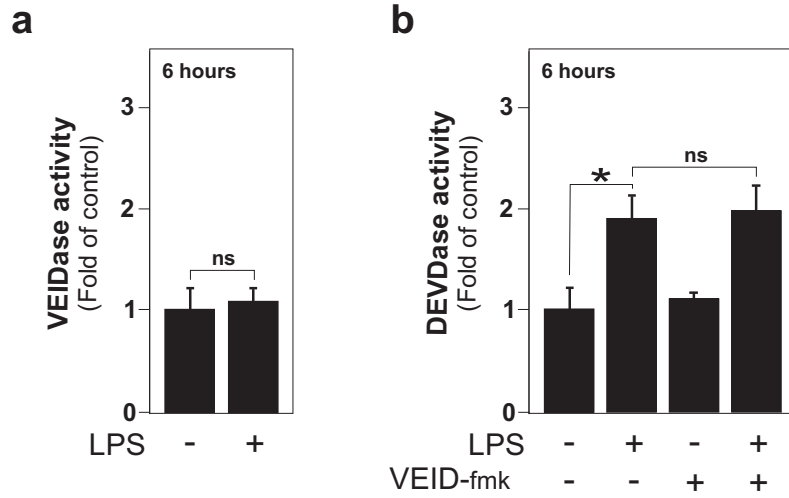


Fig S10. Burguillos et al

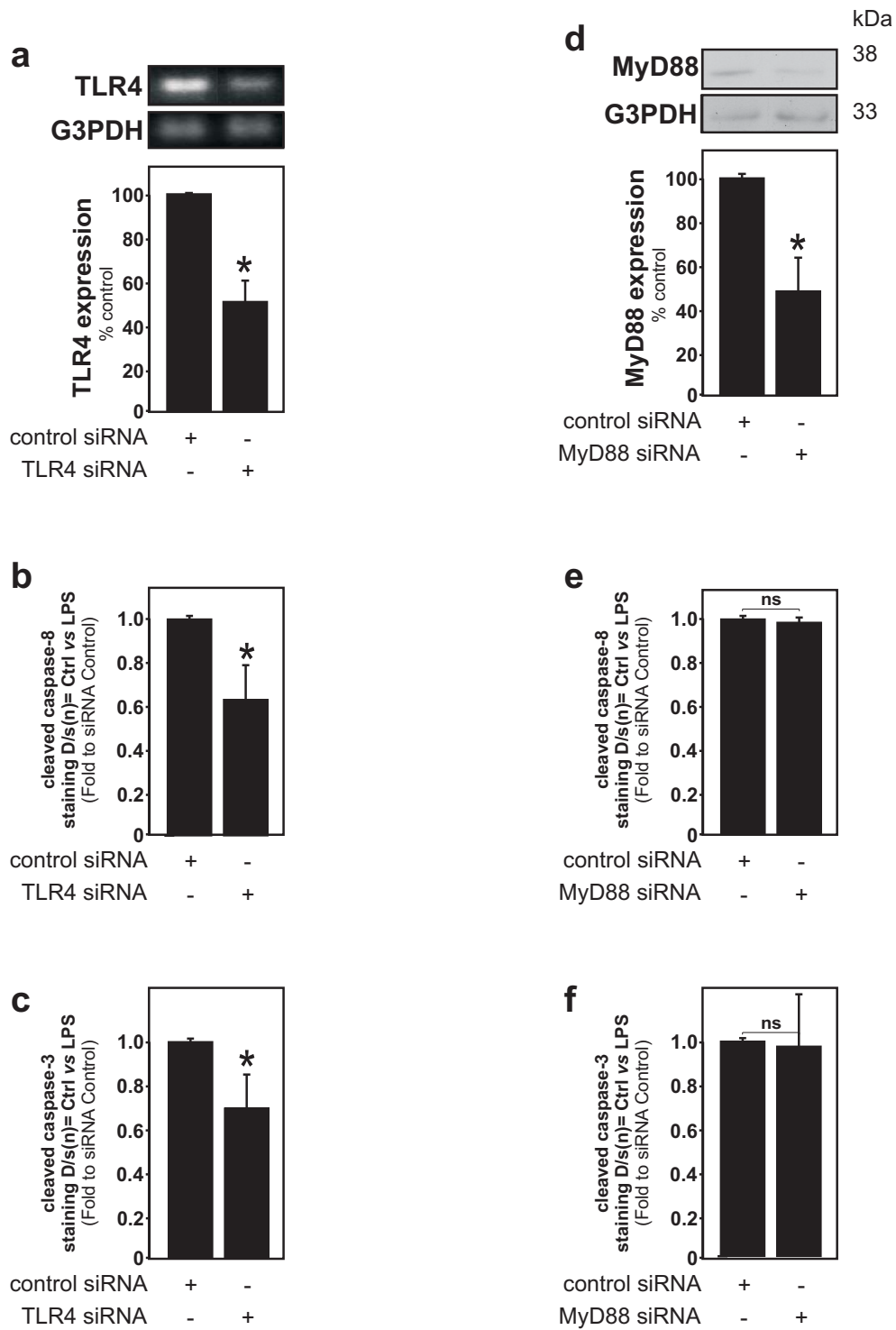


Fig S11. Burguillos et al

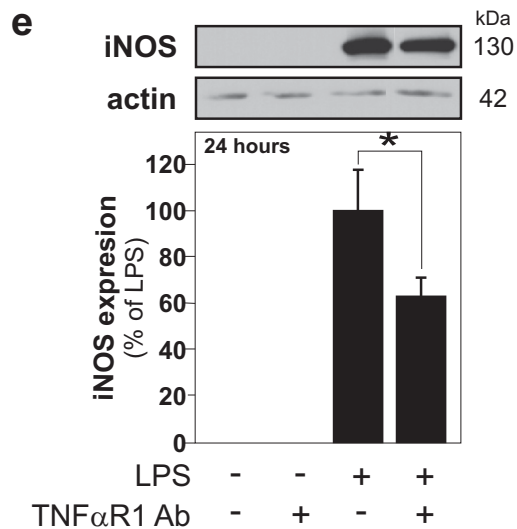
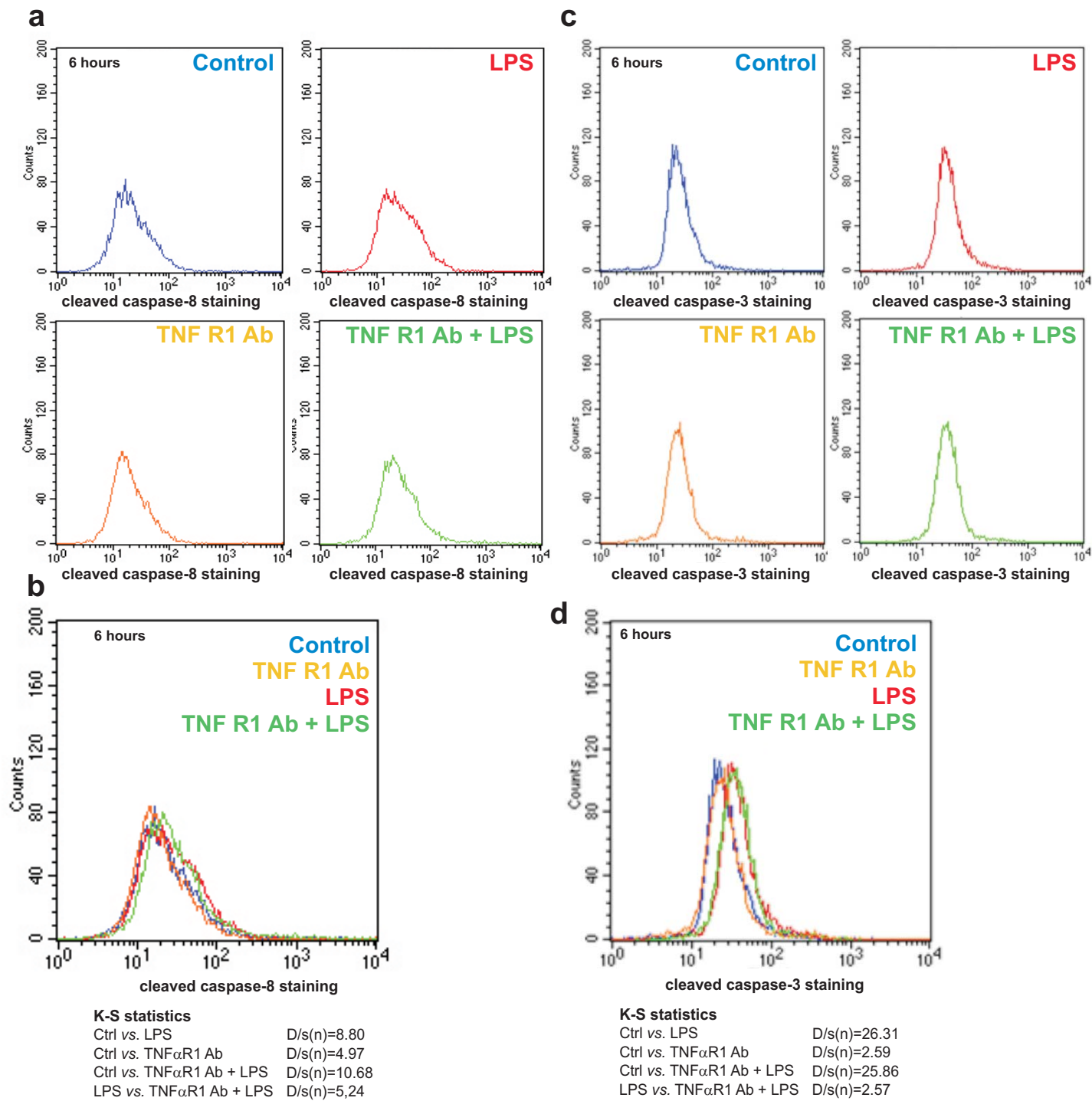


Fig S12. Burguillos et al

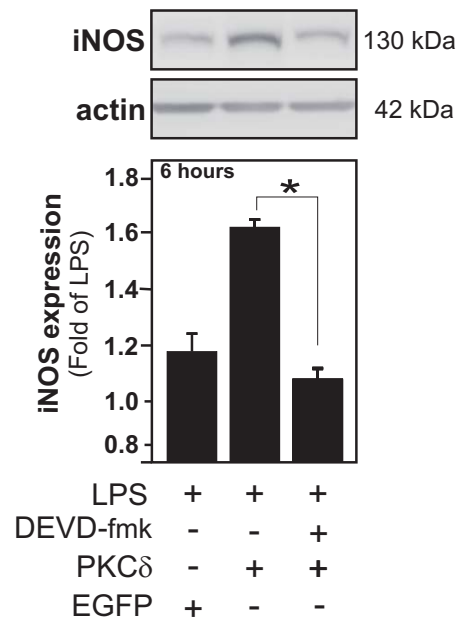


Fig S13. Burguillos et al

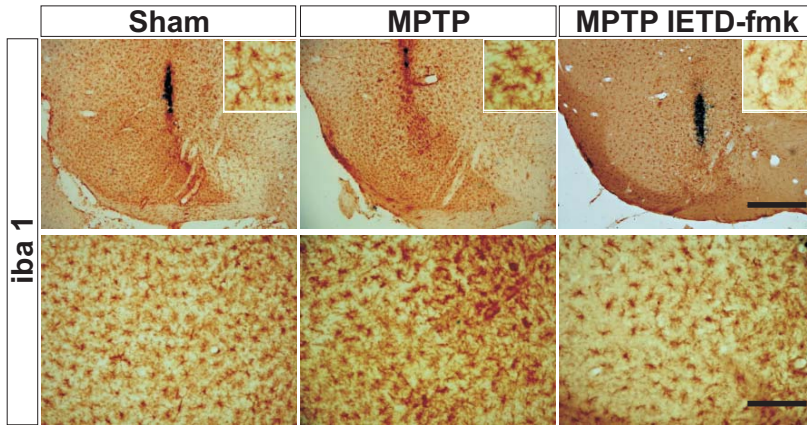
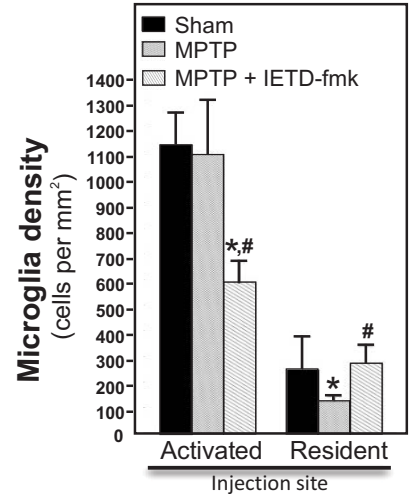
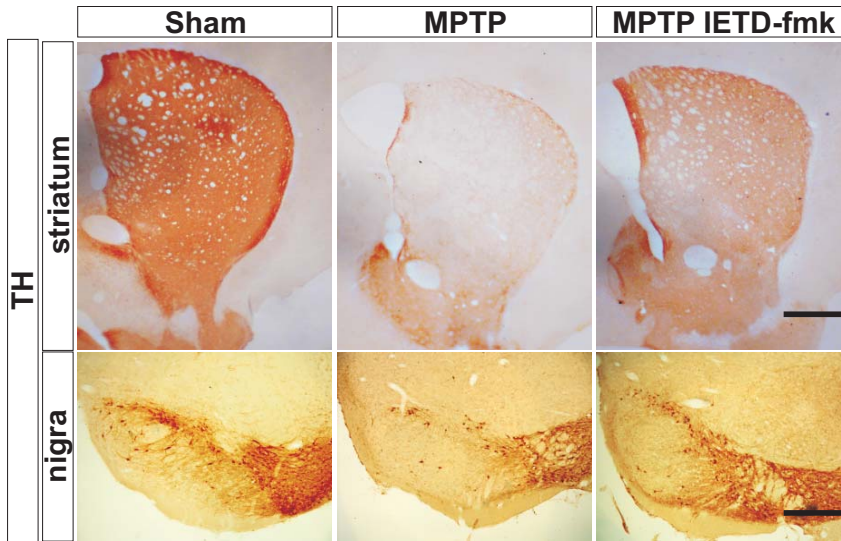
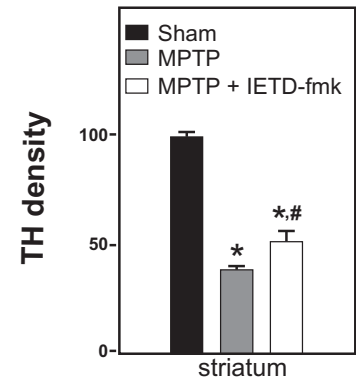
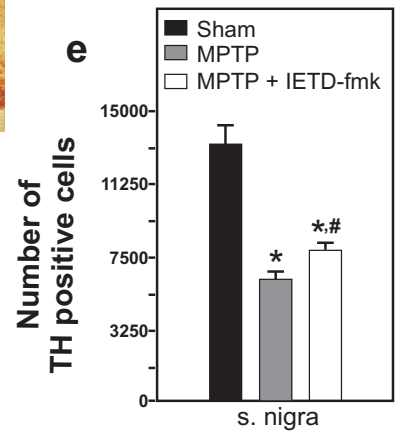
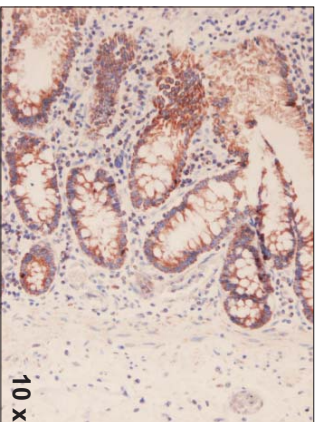
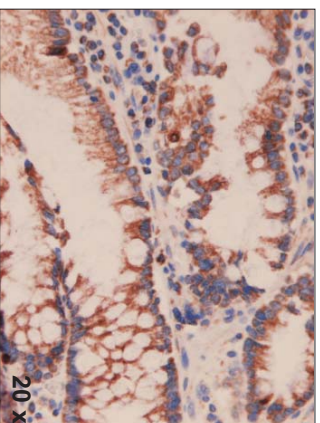
a**b****c****d****e**

Fig S14. Burguillos et al

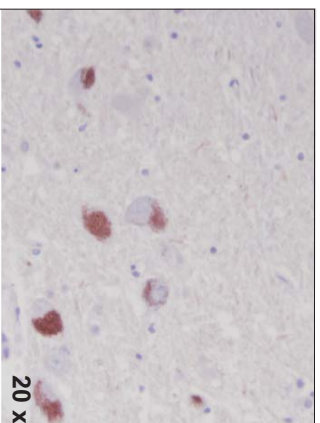
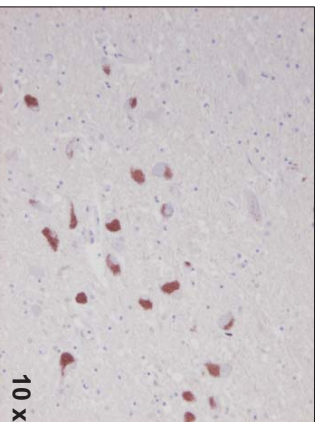
cleaved caspase-3



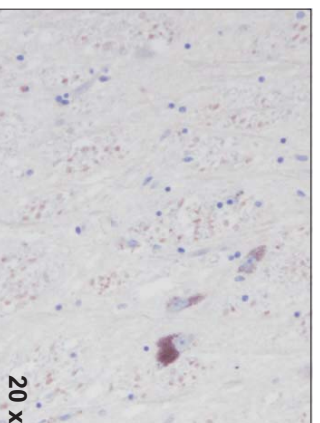
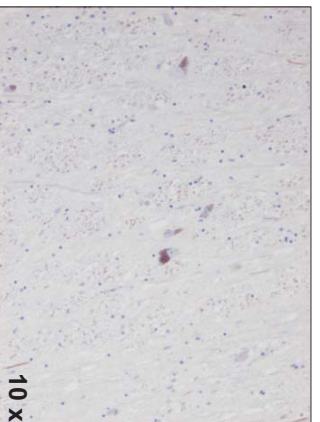
cleaved caspase-3



control case
substantia nigra



PD patient 1
substantia nigra



PD patient 2
substantia nigra

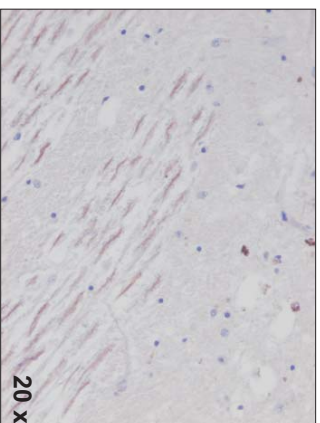
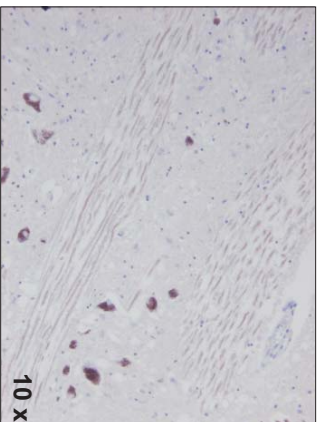
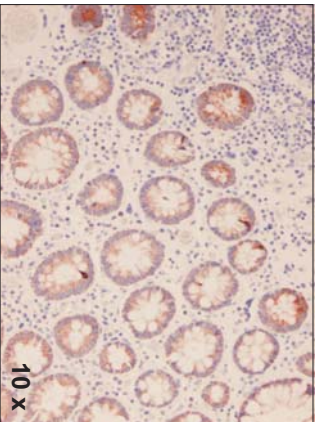


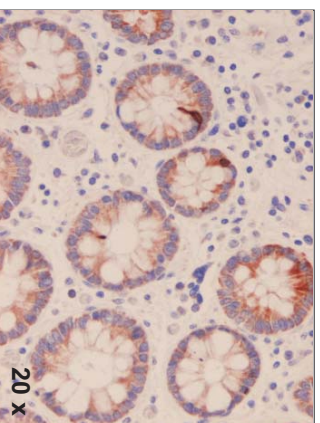
Fig S15. Burguillos et al

cleaved caspase-8

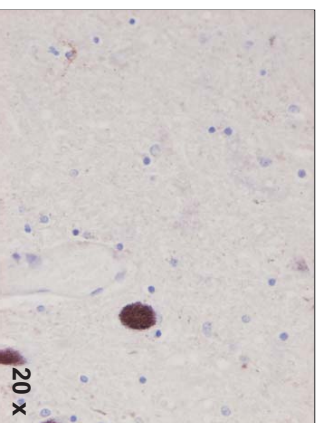
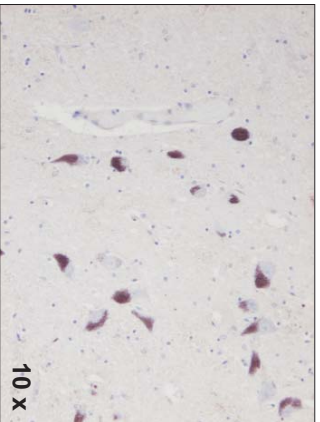
positive control
colonic mucosa



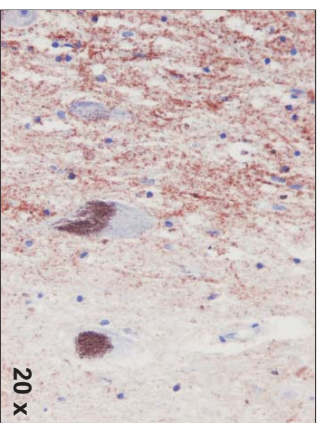
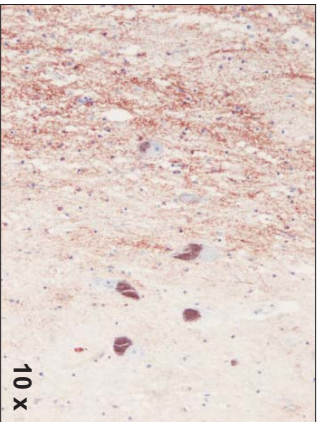
cleaved caspase-8



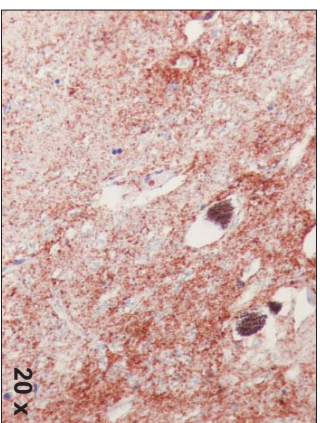
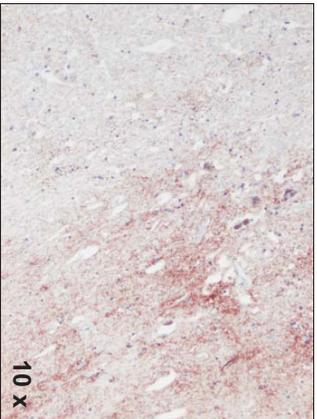
control case
substantia nigra



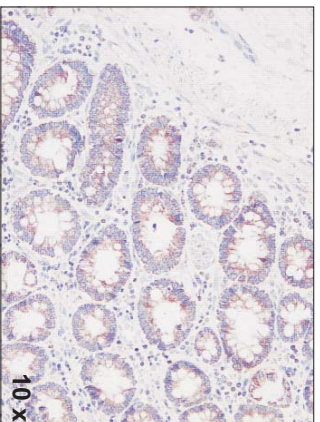
PD patient 1
substantia nigra



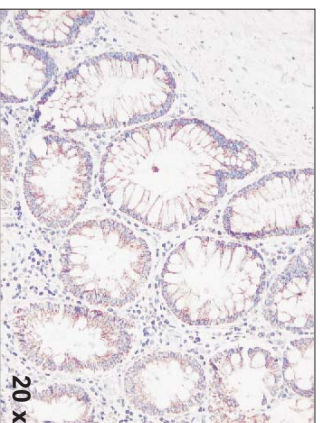
PD patient 2
substantia nigra



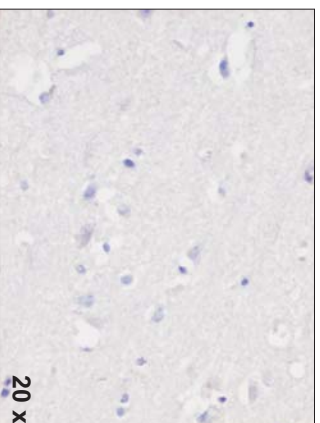
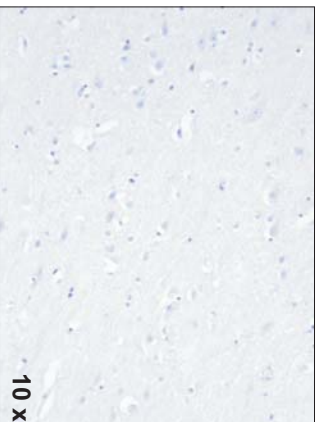
cleaved caspase-3



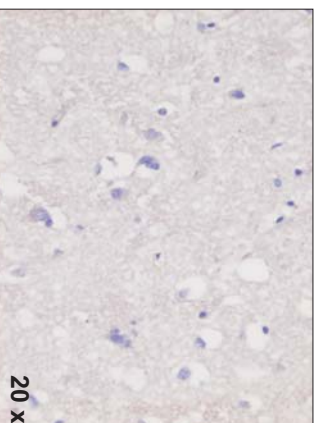
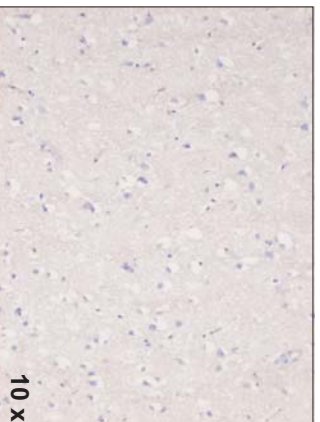
cleaved caspase-3



control case
frontal cortex



AD patient 1
frontal cortex



AD patient 2
frontal cortex

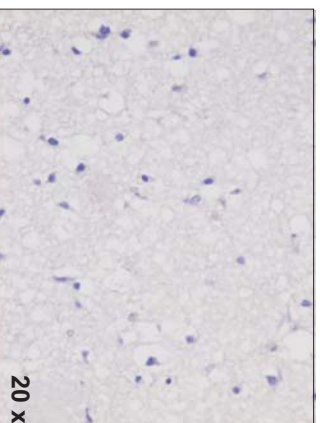
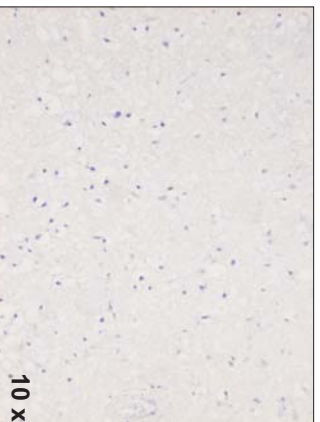
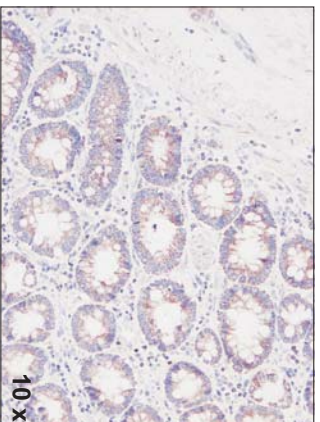
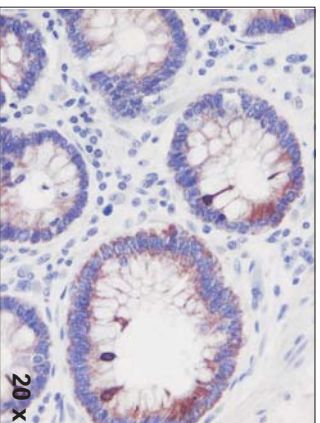


Fig S17. Burguillos et al

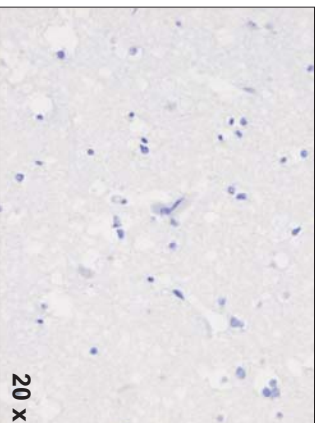
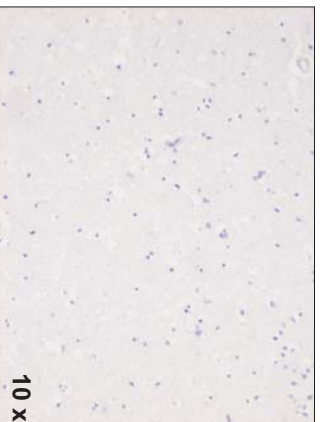
cleaved caspase-8



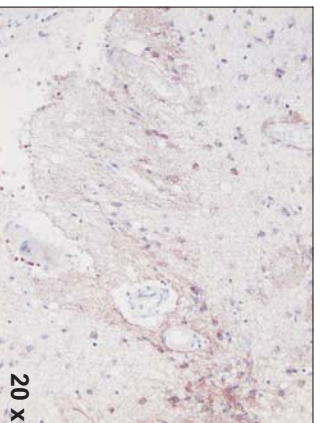
cleaved caspase-8



control case
frontal cortex



AD patient 1
frontal cortex



AD patient 2
frontal cortex

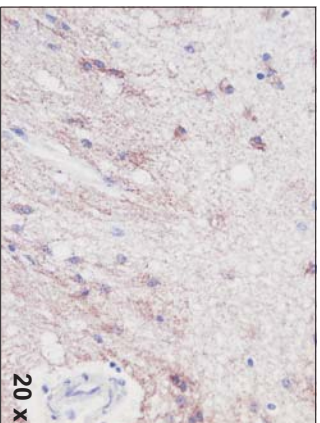
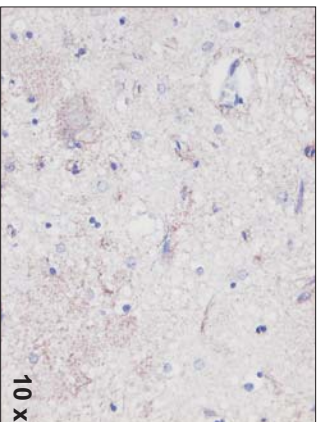
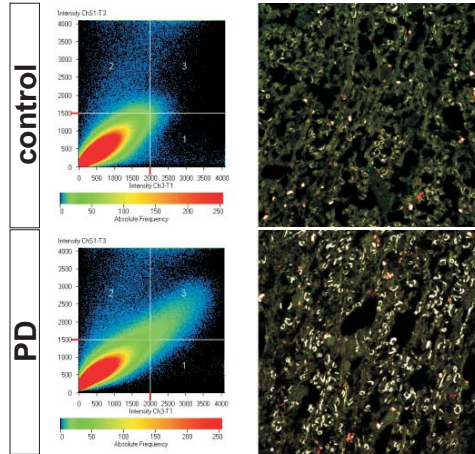


Fig S18. Burguillos et al

a **cleaved casp. 3/CD68 colocalisation**



b **cleaved casp. 8/CD68 colocalisation**

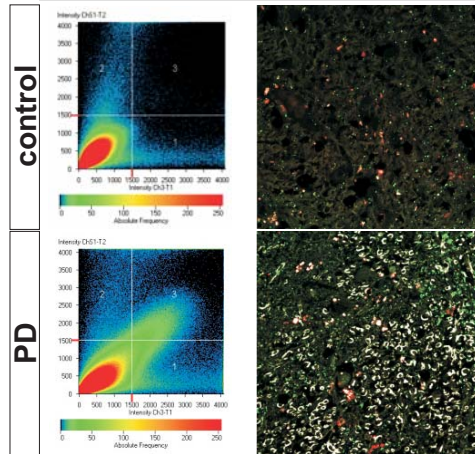


Fig S19. Burguillos et al